Progress in Neuropsychopharmacology & Biological Psychiatry 127 (2023) 110830

Contents lists available at ScienceDirect

Progress in Neuropsychopharmacology & Biological Psychiatry

journal homepage: www.elsevier.com/locate/pnp

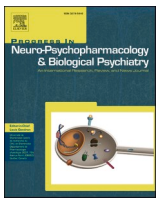

Metabolic profiling of Alzheimer's disease: Untargeted metabolomics analysis of plasma samples

Tina Milos [a], David Rojo [b], Gordana Nedic Erjavec [a,1], Marcela Konjevod [a], Lucija Tudor [a], Barbara Vuic [a], Dubravka Svob Strac [a], Suzana Uzun [c,d], Ninoslav Mimica [d], Oliver Kozumplik [d], Coral Barbas [b], Neven Zarkovic [a], Nela Pivac [a,e,*,1], Matea Nikolac Perkovic [a,*]

[a] Division of Molecular Medicine, Ruder Boskovic Institute, Zagreb, Croatia
[b] Centro de Metabolómica y Bioanálisis (CEMBIO), Facultad de Farmacia, Universidad San Pablo CEU, CEU Universities Madrid, Spain
[c] School of Medicine, University of Zagreb, Zagreb, Croatia
[d] Department for Biological Psychiatry and Psychogeriatrics, University Psychiatric Hospital Vrapče, Zagreb, Croatia
[e] University of Applied Sciences Hrvatsko Zagorje Krapina, Krapina, Croatia

ARTICLE INFO

Keywords:
Alzheimer's disease
Mild cognitive impairment
Metabolomics
Untargeted
Plasma

ABSTRACT

Alzheimer's disease (AD) is often not recognized or is diagnosed very late, which significantly reduces the effectiveness of available pharmacological treatments. Metabolomic analyzes have great potential for improving existing knowledge about the pathogenesis and etiology of AD and represent a novel approach towards discovering biomarkers that could be used for diagnosis, prognosis, and therapy monitoring. In this study, we applied the untargeted metabolomic approach to investigate the changes in biochemical pathways related to AD pathology. We used gas chromatography and liquid chromatography coupled to mass spectrometry (GC–MS and LC-MS, respectively) to identify metabolites whose levels have changed in subjects with AD diagnosis ($N = 40$) compared to healthy controls ($N = 40$) and individuals with mild cognitive impairment (MCI, $N = 40$). The GC–MS identified significant differences between groups in levels of metabolites belonging to the classes of benzene and substituted derivatives, carboxylic acids and derivatives, fatty acyls, hydroxy acids and derivatives, keto acids and derivatives, and organooxygen compounds. Most of the compounds identified by the LC-MS were various fatty acyls, glycerolipids and glycerophospholipids. All of these compounds were decreased in AD patients and in subjects with MCI compared to healthy controls. The results of the study indicate disturbed metabolism of lipids and amino acids and an imbalance of metabolites involved in energy metabolism in individuals diagnosed with AD, compared to healthy controls and MCI subjects.

1. Introduction

Dementia is a broad term which describes a group of symptoms related to disturbances in memory, thinking and social abilities, all caused by different diseases that affect the brain. The major cause of dementia in older adults is Alzheimer's disease (AD). Taking into account the current demographic trend where life expectancy of the population is constantly increasing, one can expect that in the near future AD will become one of the leading medical, social, and economic burdens of all modern societies. Unfortunately, AD is often unrecognized or diagnosed too late, which significantly reduces the effectiveness of treatment with cholinesterase inhibitors and/or memantine. Specifically, the diagnosis of AD requires excluding all other pathologies that could be the cause of dementia symptoms by combining various neuroimaging, neuropsychological, and laboratory tests (Zvěřová, 2019). The disadvantage with this kind of approach is that it is mainly effective in patients who already have significant cognitive impairment, making it difficult to diagnose people in the early stages of the disease and thus

* Corresponding authors at: Ruder Boskovic Institute, Bijenicka Cesta 54, Zagreb HR-10000, Croatia.
E-mail addresses: tina.milos@irb.hr (T. Milos), david.rojoblanco@ceu.es (D. Rojo), gnedic@irb.hr (G. Nedic Erjavec), mkonjev@irb.hr (M. Konjevod), ltudor@irb.hr (L. Tudor), barbara.vuic@irb.hr (B. Vuic), dsvob@irb.hr (D. Svob Strac), suzana.uzun@bolnica-vrapce.hr (S. Uzun), ninoslav.mimica@bolnica-vrapce.hr (N. Mimica), oliver.kozumplik@bolnica-vrapce.hr (O. Kozumplik), cbarbas@ceu.es (C. Barbas), zarkovic@irb.hr (N. Zarkovic), npivac@irb.hr (N. Pivac), mnikolac@irb.hr (M. Nikolac Perkovic).

[1] Nela Pivac, Associate Editor, and Gordana Nedic Erjavec, Guest Editor, were made blind to the reviewing process of this manuscript.

https://doi.org/10.1016/j.pnpbp.2023.110830
Received 23 April 2023; Received in revised form 7 June 2023; Accepted 11 July 2023
Available online 16 July 2023

resulting in the reduction of treatment efficiency with cholinesterase inhibitors and/or memantine. The identification of new AD biomarkers is essential for the elucidation of molecular mechanisms related to the pathogenesis and progression of this disease, the development of more reliable diagnostic tests and new therapeutic approaches. Numerous studies have shown that pathological processes associated with AD can manifest, not only in the central nervous system, but also at the periphery (Rani et al., 2017). These discoveries emphasized the importance of finding peripheral, non-invasive and easily accessible biomarkers that will enhance the development of new diagnostic tests (Zvěřová, 2019).

Metabolomics is one of the "omics" approaches that enables the monitoring of changes occurring downstream of genomic, transcriptomic and proteomic modifications. Detecting the level of endogenous metabolites, which represent the end point of all biochemical reactions, could be used as a fairly sensitive measure of an individual's overall health status. Metabolomic analyzes have a great potential for improving the existing knowledge about the pathogenesis and etiology of AD and represent a new approach towards discovering biomarkers that could be used for diagnosis, prognosis and therapy monitoring in patients with AD (Wilkins and Trushina, 2017). Such a holistic approach is crucial particularly in the case of multifactorial disorders such as AD. Untargeted metabolomic analysis enables the determination of entire metabolomic profiles without a pre-set hypothesis and it has an excellent potential for discovering new biomarkers of certain pathological conditions. In the case of AD, it is expected that people diagnosed with this type of dementia have a disturbed metabolism of lipids and amino acids and an imbalance of metabolites involved in the energy metabolism (Huo et al., 2020; Konjevod et al., 2021).

In this study, we used the untargeted metabolomic approach (Fig. 1) to investigate changes in biochemical pathways related to the pathology of AD, with the purpose of finding new and easily accessible indicators of the processes underlying this disease. We used gas chromatography coupled to mass spectrometry (GC–MS) and liquid chromatography coupled to electrospray ionization mass spectrometry (LC-MS ESI) in order to identify metabolites whose levels have changed in subjects with AD diagnosis compared to healthy controls and individuals with mild cognitive impairment (MCI). Experimental design and metabolomics workflow are presented in Fig. 1. We hypothesized that the study would offer new, easily accessible biochemical biomarkers for aiding the diagnosis of AD.

2. Materials and methods

2.1. Participants

Out of 120 subjects included in the study, 40 of them were healthy controls, 40 subjects with MCI, and 40 patients with AD. All subjects were recruited at the University Psychiatric Hospital Vrapce (Zagreb, Croatia).

The subjects with AD were diagnosed according to DSM-5 criteria (APA, 2013) and the criteria of the National Institute of Neurological and Communication Disorders and Stroke, which is part of the American National Institute of Health (NINCDS-ADRDA; National Institute of Neurological and Communicative Disorders and Stroke and Alzheimer's Disease and Related Disorders Association) (McKhann et al., 2011). Subjects with MCI were diagnosed using the criteria defined by Petersen and colleagues (Petersen et al., 2018) and by Albert and colleagues (Albert et al., 2011). Cognitive impairment was evaluated using a Mini-Mental State Examination (MMSE) test (Arevalo-Rodriguez et al., 2015).

The subjects with MCI or AD were all in- and out-patients who have signed written informed consent and have undergone neurological examination, thyroid function examination, and serologic tests for Lyme disease and syphilis. The levels of vitamin B12 and B9 were also determined for the participants included in the study. The subjects were not related to each other and had not been previously prescribed with

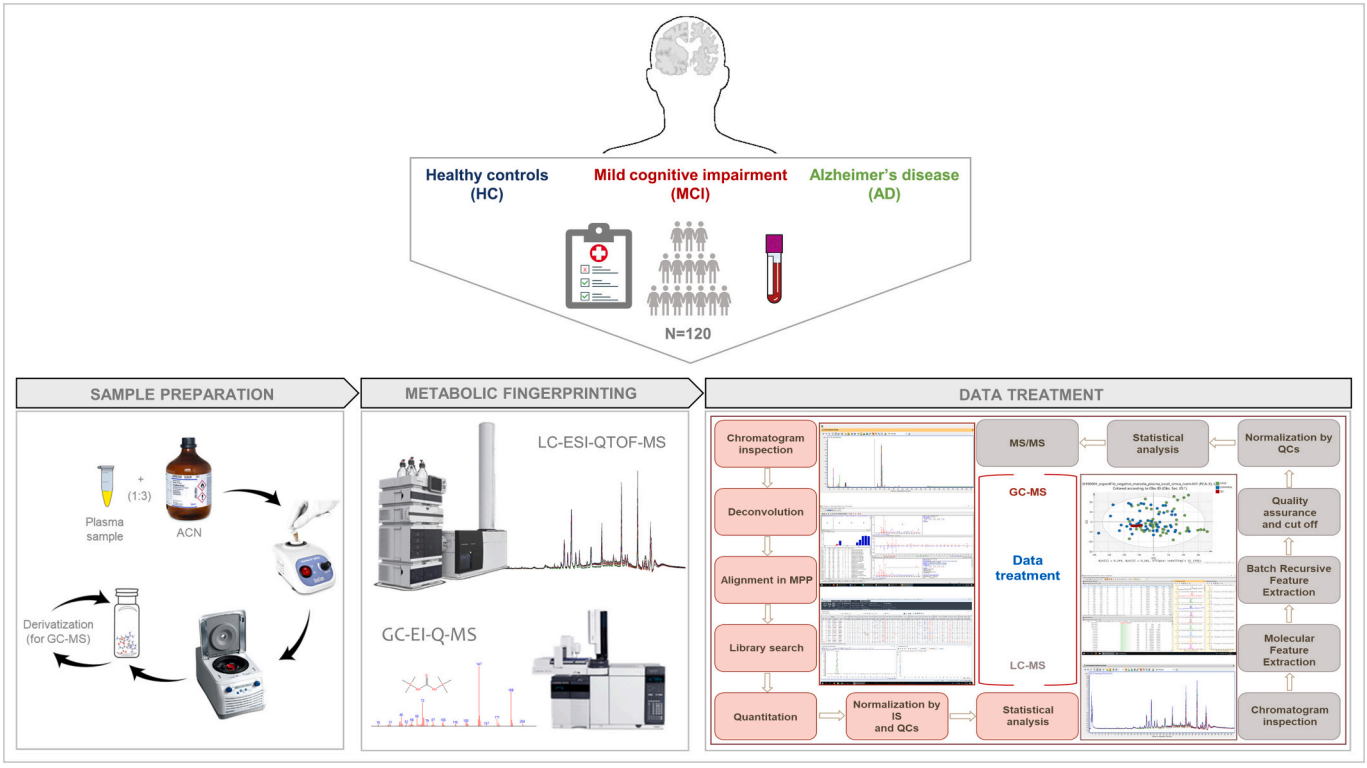

Fig. 1. Experimental design and metabolomic workflow of the study.
The workflow includes sample collection, sample preparation and metabolite extraction for both GC–MS and LC-MS, multiplatform untargeted metabolomic analysis, data treatment, statistical analyses, identification of the compounds and interpretation of the results.

any antidementia medication (cholinesterase inhibitors and/or memantine). Demographic and clinical parameters are shown in Table 1. Subjects diagnosed with vascular or mixed dementia, tumors or inflammatory diseases of the central nervous system, cardiovascular diseases, brain trauma, systemic metabolic diseases (e.g., hypertension, diabetes mellitus, obesity), and other psychiatric or neurological diseases (e.g., Huntington's disease, frontotemporal dementia) were excluded from the study. Healthy control subjects with no pathophysiological changes in the liver, following the same exclusion criteria as patients with AD or MCI, were also evaluated by the psychiatrist in order to make sure they do not have any neuropsychiatric disorder and were not treated with psychotropic medication.

The study was approved by the Ethics Committee of University Psychiatric Hospital Vrapce, Zagreb, Croatia (approval code 23–605/3–18; March 23, 2018) and carried out in line with the Helsinki Declaration (World Medical Association, 2013). All subjects have signed informed consent prior to participating in the study and the study procedures were explained in details to the participants and/or their caregivers.

2.2. Blood sample collection

Blood sampling was carried out during routine laboratory examination and after an overnight fast. Blood (8.5 mL) was drawn into yellow-top BD Vacutainer™ tubes (Becton, Dickinson and Company, Franklin Lakes, NJ, USA) with 1.5 mL of acid citrate dextrose anticoagulant. Plasma was separated using centrifugation (3 min at 1100 x*g*, followed by 15 min at 5030 ×*g*) and samples were aliquoted and stored at −80 °C until further analysis.

2.3. Metabolite extraction

2.3.1. Chemicals and reagents

For metabolomics analyses were used: acetonitrile (ACN) (LC-MS grade, Sigma-Aldrich, Steinheim, Germany), formic acid (FA) (MS grade, Sigma-Aldrich, Steinheim, Germany), heptane (Sigma-Aldrich, Steinheim, Germany), O-methoxyamine hydrochloride (Sigma-Aldrich, Steinheim, Germany), *N*,*O*-bis(trimethylsilyl) trifluoroacetamide (BSTFA) with 1% trimethylchlorosilane (TMCS) (Pierce Chemical Co, Rockford, IL, USA), and pyridine (Sigma-Aldrich, Steinheim, Ger-many). Ultrapure water was obtained from MilliQ®plus185 system (Millipore, Billerica, MA, USA). Tricosane (Sigma-Aldrich, Steinheim, Germany) and 4-chlorophenol (Sigma-Aldrich, Steinheim, Germany) were used as internal standards in GC–MS analysis. The FAME mix (mix of fatty acid methyl esters; methyl caprylate, methyl caprate, methyl laurate, methyl myristate, methyl palmitate, methyl heptadecanoate, methyl oleate, methyl stearate, methyl eicosanoate, methyl docosanoate) for GC–MS analytical platform was purchased from Supelco (Bellefonte, PA, USA). Ammonium trifluoroacetate (TFA(NH_4)), purine, and hexakis (1H,1H,3H-tetrafluoropropoxy)phosphazine (HP) from API-TOF reference mass solution kit (Agilent) were diluted in 95:5 of ACN to water ratio and used as reference solution in LC-MS analysis.

Table 1
Demographic and clinical characteristics of healthy subjects and individuals diagnosed with MCI or AD. All data are presented as median (range).

	Subjects			Kruskal-Wallis ANOVA df = 2	
	HC (N = 40)	MCI (N = 40)	AD (N = 40)	p	H
Age (years)	69.0 (65.0–77.0)	74.0 (67.0–87.0)	78.0 (67.0–89.0)	<0.001	53.55
BMI (kg/m2)	30.5 (23.0–37.0)	22.0 (18.0–29.0)	23.4 (19.0–32.0)	<0.001	42.75
Total cholesterol (mmol/l)	4.5 (2.9–7.8)	5.7 (3.2–8.8)	5.8 (3.2–8.8)	0.051	5.95
HDL-cholesterol (mmol/l)	1.2 (0.5–2.0)	1.4 (0.7–3.0)	1.3 (0.7–3.0)	0.090	4.81
LDL-cholesterol (mmol/l)	2.8 (1.3–5.4)	3.1 (0.8–4.9)	3.3 (0.8–5.8)	0.311	2.33
Triglycerides	1.6 (0.6–3.7)	1.9 (0.8–6.7)	1.9 (0.8–6.7)	0.176	3.48
Blood glucose (mmol/l)	5.0 (3.4–10.2)	5.5 (4.5–11.8)	5.7 (4.7–11.8)	0.008	9.58
MMSE score	30.0 (29.0–30.0)	27.0 (24.0–28.0)	14.0 (9.0–23.0)	<0.001	107.37

AD, Alzheimer's disease; HC; healthy controls; HDL, high-density lipoproteins; BMI, body mass index; LDL, low-density lipoproteins; MCI, mild cognitive impairment; MMSE, mini-mental state examination.

2.3.2. Preparation of samples for GC–MS analysis

For the GC–MS analysis, the samples were first deproteinized by mixing 100 μL of each plasma sample with 300 μL of cold ACN (1:3 ratio). The samples were vortex-mixed for 2 min and incubated on ice for 5 min. The aliquot of each sample (100 μL) was centrifuged (16,000 x*g*, 10 min, 4 °C), the supernatant was transferred to the crimp top clear glass vials with insert, and 20 μL of 4-chlorophenol (100 ppm, in ACN) was added. The samples were evaporated to dryness using a Speedvac Concentrator (Thermo Fisher Scientific, Waltham, MA). Methoximation was performed by adding 10 μL of O-methoxyamine hydrochloride (15 mg/mL, in pyridine). The samples were vigorously vortex-mixed for 5 min, followed by three cycles of ultrasonication (2 min) and vortex mixing (2 min). Afterwards, the vials were incubated in the dark at room temperature for 16 h. The next day, 10 μL of BSTFA with 1% TMCS was added to each vial for silylation, the samples were vortex-mixed for 5 min, and the silylation was carried out at 70 °C for 1 h. After the samples cooled down, 100 μL of tricosane (20 ppm, in heptane) was added as an internal standard and the samples were vortex-mixed for 2 min. Blank samples (ACN to water ratio 3:1) were prepared in the same way as plasma samples. Individual quality control samples (QCs) were prepared by pooling and mixing equal volumes of each plasma sample (10 μL). They were processed in the same way as the plasma samples following all the steps previously described.

2.3.3. Preparation of samples for LC-MS analysis

On the day of analysis, the plasma samples were slowly defrosted on ice and vortex-mixed for 2 min. For metabolite extraction, 100 μL of each sample was mixed with cold ACN (1:3 ratio), vortex-mixed for 2 min and incubated on ice for 5 min. After centrifugation (16,000 x*g*, 10 min, 4 °C), the remaining supernatant (200 μL) was transferred to the crimp top clear glass vials with an insert. Individual QCs were prepared by pooling and mixing equal volumes of each plasma sample (10 μL). They were processed in the same way as the plasma samples following all the steps previously described. Blank samples (ACN to water ratio 3:1) were also prepared in the same way as plasma samples.

2.4. Metabolomic fingerprinting

2.4.1. GC–MS analysis

For the metabolomic fingerprinting of plasma samples, the Agilent 7890A gas chromatograph, with an autosampler (Agilent Technologies 7693), coupled to an inert MSD with Quadrupole (Agilent Technologies 5975) was used. For each sample, a volume of 2 μL was injected, with a split ratio 1:10, into a Restek 20,782 deactivated glass-wool split liner. Compounds were separated using the GC-Column DB-5MS (length: 30 m, internal diameter: 0.25 mm, film thickness: 0.25 μm, packing: 95% dime-thylpolysiloxane/5% diphenylpolysiloxane) with a pre-column (10 m J&W integrated with Agilent 122–5532G). The constant flow rate of the helium carrier gas was set to 1 mL/min, and the injector temperature was kept constant at 250 °C. The temperature of the column oven was set at 60 °C (held for 1 min), with an increased rate of 10 °C/

min until the temperature reaches 325 °C. The temperature was maintained for up to 10 min before the injection of the next sample. The detector transfer line was set at 290 °C, while the filament source and quadrupole temperatures were set at 230 °C and 150 °C, respectively. The total analysis for each sample lasted 37.5 min. The electron ionization (EI) energy was set to 70 eV. The system collected the mass spectra in a mass range between 50 and 600 *m/z*, at a rate of 2 spectra/s.

2.4.2. LC-MS analysis

The liquid chromatography system, Agilent Technologies Series 1200 binary solvent delivery system (Agilent Technologies, Waldbronn, Germany), comprised of a binary pump, an integrated degasser, and an autosampler with a thermostat, coupled to an Agilent 6520 Accurate-Mass Q-TOF detector, was used to analyze the metabolic profile of the samples. For the separation of metabolites, a reversed-phase column (Discovery® HS C18 HPLC Column, 515 cm × 2.1 mm, 3 μm; Supelco, USA) with a pre-column (Discovery® HS C18 HPLC Column, 2 cm × 2.1 mm, 3 μm; Supelco, USA), was used and kept at 60 °C during the analysis. The injection volume was set at 10 μL. The elution conditions employed a flow rate of 0.6 mL/min with a gradient of the solvent A (H_2O with 0.1% FA) and the solvent B (ACN with 0.1% FA). The analysis started with 25% of the mobile phase B and then in-creased to the 95% of B in a time period of 35 min (0–35 min). The gradient then returned to the initial conditions in 1 min time (35–36 min), 25% of the mobile phase B, and these conditions were maintained until the end of the analysis (36–45 min). All the samples were analyzed in both positive and negative ESI mode (full-scan ranging from 50 to 1000 m/z), with a scan rate of 1.02 scans/s. Two reference masses were continuously infused during the entire duration of the analysis to ensure a constant mass correction: 121.0509 (purine, detected m/z $[C_5H_4N_4 + H]^+$) and 922.0098 (HP, detected m/z $[C_{18}H_{18}O_6N_3P_3F_{24} + H]^+$) for the positive mode, and 112.9855 (TFA(NH_4), detected m/z $[C_2O_2F_3(NH_4)\text{-}H]^-$) and 966.0007 (HP + FA, detected m/z $[C_{18}H_{18}O_6N_3P_3F_{24} + \text{FA-}H]^-$) for the negative mode.

Tandem mass spectrometry (MS/MS) was performed to facilitate the identification of significant metabolites, using the same LC-MS platform and the same chromatographic conditions as applied for the primary LC-MS analysis. The selected ions were targeted for fragmentation by collision-induced dissociation (CID) based on the previously determined accurate mass and retention time. Multiple collision energies (10 eV, 20 eV, and 40 eV) were used.

2.5. Data treatment and metabolite identification

2.5.1. GC–MS

The quality of the total ion chromatograms (TIC) for all analyzed samples, QCs, and blanks was assessed using Agilent MassHunter Quantitative Analysis software, version B.07.00. After checking the reproducibility of the signals of the internal standards (4-chlorophenol for derivatization and tricosane for analytical performance), all the samples were accepted. The raw data files were imported into the Agilent Mas-sHunter Unknowns Analysis software (version B.09.00) for deconvolution and identification of the compounds using targeted libraries (Fiehn library version 2013, and the in-house CEMBIO spectral library for plasma samples). The compounds were identified based on their retention time (RT) and mass spectra. Additionally, the identified compounds and the non-identified features were reevaluated using the NIST library (National Institute of Standards and Technology, library 2.2 version 2014). Obtained data was aligned with the Agilent MassProfiler Professional software (version 13.0) and exported into Agilent MassHunter Quantitative Analysis (version B.09.00) for peak integration. The abundance of each compound in the obtained data matrix was normalized according to the tricosane (internal standard) abundance, and the blank subtraction was performed prior to statistical analysis.

2.5.2. LC-MS

The quality of the analysis was assessed using Agilent MassHunter Quantitative Analysis software, version B.07.00. by inspecting total ion chromatograms (TIC), checking the pressure curves in order to assess the stability of chromatographic conditions, and reviewing the stability of the reference masses' signal for each sample, QCs and blanks. All the samples have passed all the check points. Afterwards, the raw data were imported into Agilent MassHunter Profinder software (version B.08.00) for deconvolution. The Molecular Feature Extraction (MFE) algorithm was used for deconvolution, creating a list of possible molecular features that matches a Gaussian distribution of coeluting ions related by charge-state, isotopic distribution and/or the presence of different adducts, and dimmers. A second deconvolution step was performed by the Recursive Feature Extraction (RFE) algorithm, which reintegrates MFE results improving the quality of the final features list. The obtained list of statistically significant accurate masses was annotated using the CEU Mass Mediator search tool (Gil de la Fuente et al., 2018), with maximum error mass ± 20 ppm, in order to assign possible (tentative) metabolite candidates. Compounds were identified using the accurate mass and by checking their isotopic pattern. Only the features with the highest score were kept for further identity confirmation by LC-MS/MS. The biological role of each compound was also evaluated in order to exclude the unrelated and impossible identification matches. The LC-MS/MS was performed only for the statistically significant and annotated features in both positive and negative ionization mode. The final identification of these compounds was performed by matching their fragmentation spectra with the reference spectra in curated databases such as HMDB (Wishart et al., 2018), METLIN (Smith et al., 2005), KEGG (Kanehisa and Goto, 2000), and LipidMaps (Fahy et al., 2007). For compound identification we considered proper retention time, accurate mass (maximum error mass ± 20 ppm), and at least two MS/MS fragments.

2.6. Statistical analysis

Before the statistical analysis, the raw data obtained by both GC–MS and LC-MS were filtered based on the proposed criteria (Godzien et al., 2015). The variables were retained if they were present in ≥80% of the QCs (with relative standard deviation (RSD) <30% in QC samples), or if they were present in <20% of the QCs, but also present in ≥50% of the samples in a specific subject group. In order to correct for the possible intra-batch effect, we used the Quality Control-Robust Spline Correction (QC-RSC) algorithm (Kuligowski et al., 2015). Support vector regression (QC-RSC) was performed using MATLAB (7.10.0.499, MathWorks, Natick, MA, USA) and the LIBSVM library (Chang and Lin, 2011). After eliminating intra-batch effects, data was normalized in order to decrease the unwanted variations which may result from the errors in the sample preparation (De Livera et al., 2012). Auto scaling (Unit Variance, UV) was used to normalize and scale metabolic signals (Gromski et al., 2015). In case of GC–MS data, the abundance of detected compounds was additionally normalized by the signal of internal standard (tricosane) in each sample. The missing values in our data sets were replaced with zeros (Armitage et al., 2015).

For multivariate statistical analyses the SIMCA-P+ software (version 15.0.2.5959, Umetrics, Umea, Sweden) was used. This includes building up Principal Component Analysis (PCA) models, Partial Least Squares-Discriminant Analysis (PLS-DA) and Orthogonal PLS-DA (OPLS-DA) models. Based on OPLS-DA models, volcano plots plotting variable importance in the projection (VIP) against corrected *p*-values [p(corr), loading values scaled as correlation coefficients values] were obtained. Univariate statistical analyses were done using MATLAB (7.10.0.499, MathWorks, Natick, MA, USA). The normal distribution was evaluated using the Kolmogorov-Smirnov test. The comparison of metabolite abundances between specific groups (AD vs. healthy controls, MCI vs. healthy controls, and AD vs. MCI) was done using Student's *t*-test or Mann-Whitney *U* test, depending on data distribution, followed by Benjamini-Hochberg (FDR, false discovery rate) post hoc correction for

multiple comparisons. Changes in the levels of metabolites with $p \leq 0.050$ (Benjamini-Hochberg adjusted p-value obtained with univariate statistical analysis), VIP > 1.00, and absolute p(corr) ≥ 0.30 were considered significant. The percentage of change (%Δ) was calculated as follows: [(average value in the CASE group - average value in the CONTROL group)/(average value in CONTROL group)] $\times$ 100, with positive values indicating increased abundance and negative values decreased abundance of specific metabolites in the CASE group, when compared to the CONTROL group.

Demographic and clinical characteristics of the participants deviated from the normal distribution (tested with the Kolmogorov-Smirnov test); therefore, the non-parametric Kruskal-Wallis ANOVA by ranks, with Dunn's multiple post-hoc comparisons test, was used to compare the subject groups. The relationship of significantly altered metabolites with age, BMI, and blood glucose levels was evaluated using partial correlation, whilst controlling for the possible effect of diagnosis. To additionally evaluate the effect of age on altered compounds, a multilinear regression model was performed, with the level of specific metabolites as dependent variables. The first block of multilinear regression included only age as an independent variable, while the second block included both age and diagnosis as independent variables.

Metabolic pathway analysis was conducted using a freely accessible web-based metabolomics analysis platform MetaboAnalyst 5.0 (https://www.metaboanalyst.ca/, accessed on 20 April 2023). MetaboAnalyst 5.0 was used to identify and visualize the affected metabolic pathways (Pang et al., 2021).

The sample size was determined using the tool G*Power 3.1.9.2 (Faul et al., 2007). To achieve a power of 80%, with fixed $\alpha = 0.05$ and effect size $d = 0.5$, in the case of determining differences in two independent means, the total sample size needed is 34, so we decided to use groups with 40 participants in each group.

3. Results

3.1. Participants

The study included a total of 120 male participants subdivided into three groups; healthy control subjects ($N = 40$), subjects with MCI ($N = 40$) and subjects diagnosed with AD ($n = 40$). Different demographic and clinical characteristics of the participants are shown in Table 1. Since all examined demographic and clinical parameters deviated from the normal distribution, the non-parametric Kruskal-Wallis ANOVA by ranks, with Dunn's multiple post-hoc comparisons test, was used to compare different subject groups (Table 1).

Subjects differed significantly (Table 1) in age ($p < 0.001$), BMI ($p < 0.001$), blood glucose level ($p = 0.008$), and, as expected, cognitive abilities assessed with MMSE ($p < 0.001$). Namely, the patients with AD were significantly older than MCI subjects ($p = 0.003$; Dunn's post-hoc test) and healthy controls ($p < 0.001$; Dunn's post-hoc test), and participants diagnosed with MCI were older than healthy subjects ($p < 0.001$; Dunn's post-hoc test). The difference in BMI is the result of significantly lower BMI in AD ($p < 0.001$; Dunn's post-hoc test) and MCI ($p < 0.001$; Dunn's post-hoc test) subjects compared to healthy controls (Table 1). Blood glucose level was similar in MCI and healthy control group, and in AD patients and MCI subjects. However, participants diagnosed with AD had significantly higher blood glucose level than healthy subjects ($p = 0.006$; Dunn's post-hoc test). As expected, AD patients had significantly lower MMSE score compared to subjects with MCI ($p < 0.001$; Dunn's post-hoc test) and healthy controls ($p < 0.001$; Dunn's post-hoc test). In addition, individuals with MCI had more pronounced cognitive impairment than healthy subjects ($p < 0.001$; Dunn's post-hoc test). Subjects had similar total cholesterol level ($p = 0.051$), HDL- ($p = 0.090$) and LDL-cholesterol ($p = 0.311$) concentration, as well as triglyceride levels ($p = 0.176$).

3.2. Metabolomic profiling of plasma samples

Multiplatform untargeted metabolomic analysis of plasma samples revealed diverse metabolic signatures in patients diagnosed with AD, subjects with MCI and healthy controls. In order to determine the differences in metabolomic profiles of these subject groups, the PCA was used. Unsupervised PCA was used to generated the two-dimensional score plots in order to visualize the clustering of samples based on their similarity. PCA reduces the number of variables in a data set combining them into artificial variables called principal components, while preserving as much information as possible. The two first principal components describe the most variation in the dataset and they are used to visualize the general trends in the dataset using a PCA scatterplot. In our study PCA was performed for all three groups of samples (Fig. 2) and separately for all group comparisons, AD vs. healthy controls, MCI vs. healthy controls, and AD vs. MCI (Figs. 3-5).

The PCA score plot for all sample groups showed the greatest separation of data points between healthy controls and patients with AD, with data points corresponding to MCI subjects located between these two groups (Fig. 2). Smaller overlaps between data points corresponding to healthy controls and AD subjects indicate that these two groups differ more in the measured variables (Fig. 2). Larger overlaps between data points corresponding to MCI subjects and data points corresponding to healthy controls or subjects with AD indicate that the differences between these groups (healthy controls vs. MCI and MCI vs. AD) are less pronounced (Fig. 2). Tight clustering of the QC samples in all analysis validates the analytical performance and confirms that data normalization corrected all potential instrumental variation, corroborating the biological differences between the clinical groups (Figs. 2-5). After PCA, PLS-DA model was generated for all subject groups, while supervised OPLS-DA models were generated to discriminate two separate groups of samples (AD vs. healthy controls, MCI vs. healthy controls, and AD vs. MCI), and the VIP scores were used to identify those metabolites that contributed the most to the differences between groups (Tables 2-3). All generated OPLS-DA models were built from one predictive component and two orthogonal components.

Using the GC–MS analysis, a total of 88 signals was detected, while LC-MS analysis resulted in 761 features detected in the positive mode and 783 in the negative ionization mode. After normalization of raw data matrix, curation of the data, statistical analysis and metabolite identification, a total of 29 metabolites detected with GC–MS were significantly altered between AD patients, subjects with MCI and healthy controls (Table 2), while LC-MS analyses identified a total of 24 significantly altered metabolites (Table 3).

Significantly altered metabolites, detected by GC–MS, are presented in Table 2. The list of metabolites whose abundance was found to be significantly different in healthy controls compared to subjects diagnosed with AD or MCI, and/or significantly different in AD patients in comparison to individuals with MCI, was determined using the combination of multivariate and univariate statistics (Table 2). Altered compounds, detected by GC–MS, belong to benzene and substituted derivatives, carboxylic acids and derivatives, fatty acyls, hydroxy acids and derivatives, keto acids and derivatives, and organooxygen compounds (Table 2). The abundance of benzoic acid was decreased in MCI subjects compared to healthy controls and patients with AD, while the level of hippuric acid seems to increase in MCI subjects when compared to healthy controls and AD patients. Therefore, these two compounds could have potential in MCI detection. Moreover, obtained results suggest lower levels of different amino acids and their derivates (proline, valine, glycine, succinic acid, serine, threonine, pyroglutamic acid, glutamic acid) in AD patients in comparison to both healthy control subjects and MCI subjects (Table 1). The abundance of valine, succinic acid and glutamic acid was also reduced in MCI subjects compared to healthy controls, but, as mentioned before, increased in comparison to the patients with AD. Citric acid was found to be less abundant in both AD and MCI subject compared to healthy individuals; however, the level

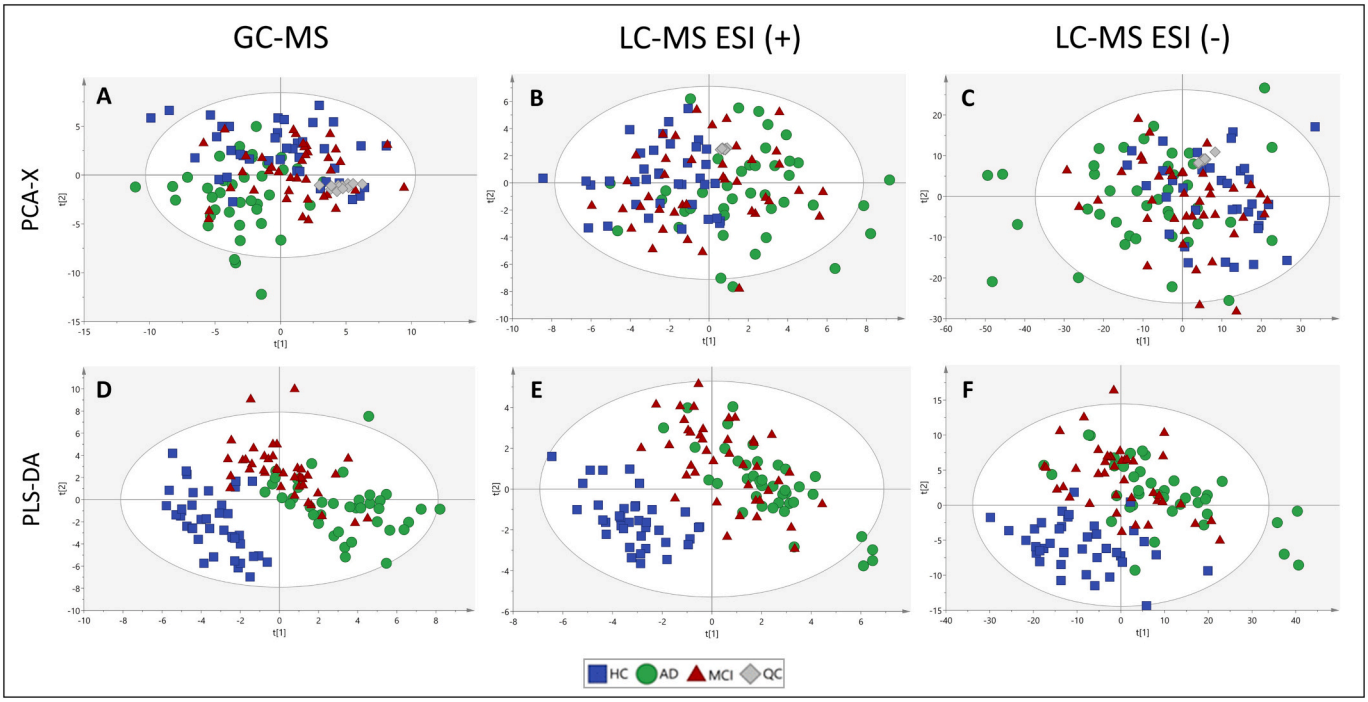

Fig. 2. PCA and PLS-DA score plots of the untargeted metabolomics analysis of plasma samples from healthy control individuals (HC), patients diagnosed with AD and subjects with MCI.
Plots were obtained using SIMCA-P+ software (version 15.0.2.5959, Umetrics, Umea, Sweden). The data matrix was pretreated using log-transformation and unit variance (UV) scaling method. (A) PCA score plot for the GC–MS analysis (R2X(cum) = 0.753); (B) PCA score plot for the LC-MS ESI (+) analysis (R2X(cum) = 0.751); (C) PCA score plot for the LC-MS ESI (−) analysis (R2X(cum) = 0.368); (D) PLS-DA score plot for the GC–MS analysis (R2 = 0.612; Q2 = 0.509); (E) PCA score plot for the LC-MS ESI (+) analysis (R2 = 0.474; Q2 = 0.408); (F) PLS-DA score plot for the LC-MS ESI (−) analysis (R2 = 0.470; Q2 = 0.285); QC = quality control.

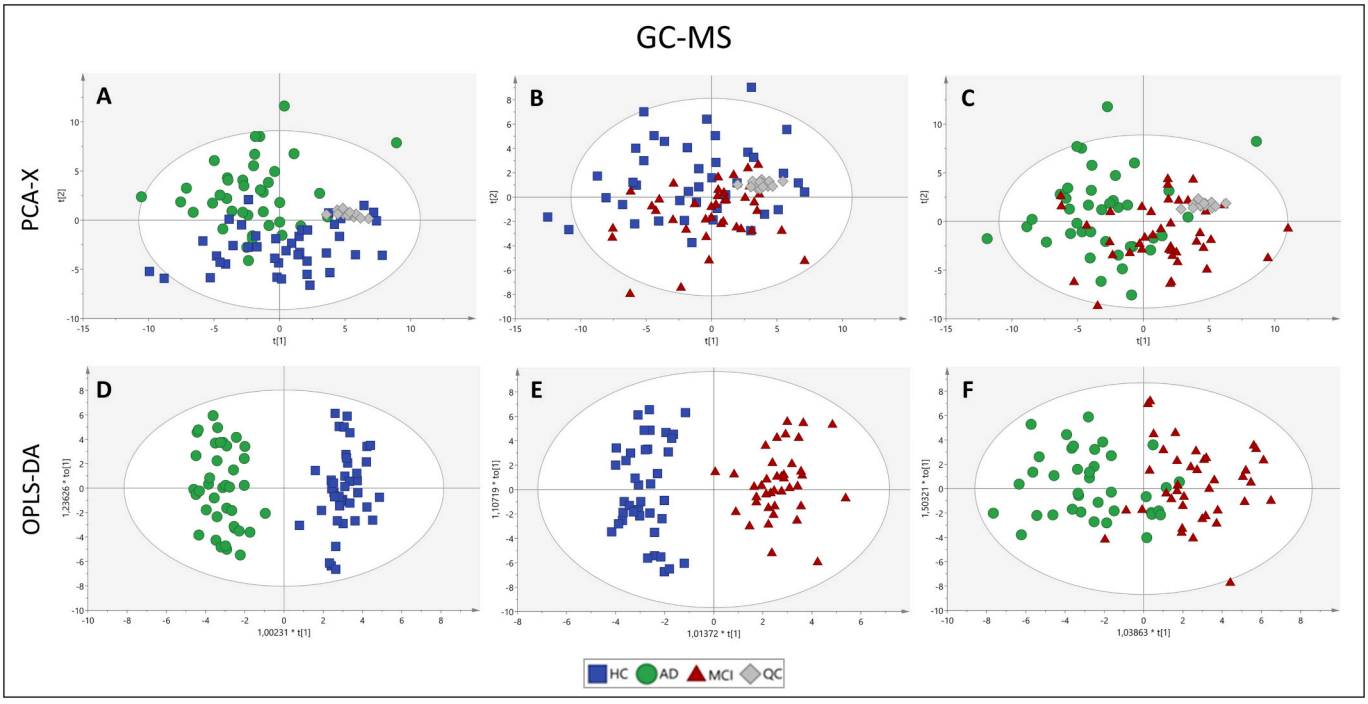

Fig. 3. PCA and OPLS-DA score plots of the untargeted metabolomics GC–MS analysis of plasma samples from healthy control individuals (HC), patients diagnosed with AD subjects with MCI.
Plots were obtained using SIMCA-P+ software (version 15.0.2.5959, Umetrics, Umea, Sweden). The data matrix was pretreated using log-transformation and unit variance (UV) scaling method. (A) PCA score plot for AD and HC subject groups (R2X(cum) = 0.753); (B) PCA score plot for MCI and HC subject groups (R2X(cum) = 0.747); (C) PCA score plot for AD and MCI subject groups (R2X(cum) = 0.791); (D) OPLS-DA score plot for AD and HC subject groups (R2 = 0.934; Q2 = 0.869); (E) OPLS-DA score plot for MCI and HC subject groups (R2 = 0.884; Q2 = 0.851); (F) OPLS-DA score plot for AD and MCI subject groups (R2 = 0.600; Q2 = 0.335); QC = quality control.

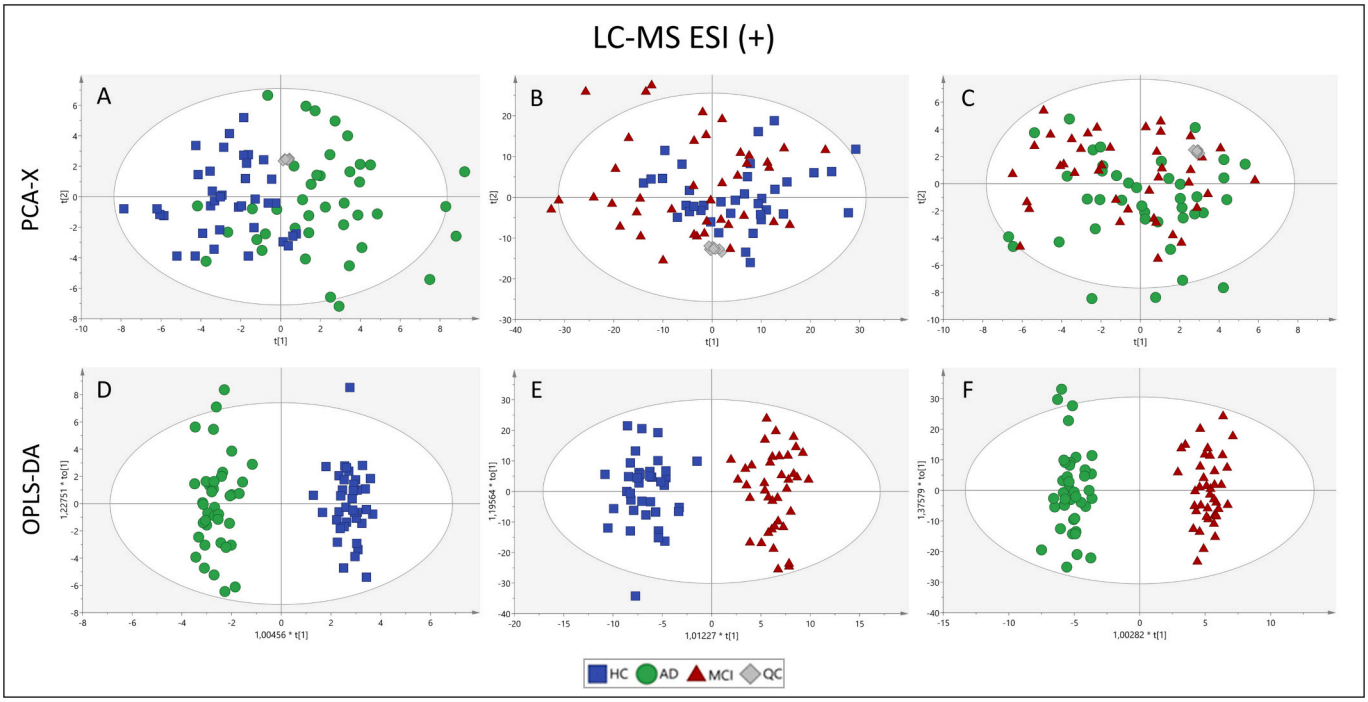

Fig. 4. PCA and OPLS-DA score plots of the untargeted metabolomics LC-MS ESI (+) analysis of plasma samples from healthy control individuals (HC), patients diagnosed with AD and subjects with MCI.
Plots were obtained using SIMCA-P+ software (version 15.0.2.5959, Umetrics, Umea, Sweden). The data matrix was pretreated using log-transformation and unit variance (UV) scaling method. (A) PCA score plot for AD and HC subject groups (R2X(cum) = 0.742); (B) PCA score plot for MCI and HC subject groups (R2X(cum) = 0.654); (C) PCA score plot for AD and MCI subject groups (R2X(cum) = 0.672); (D) OPLS-DA score plot for AD and HC subject groups (R2 = 0.963; Q2 = 0.927); (E) OPLS-DA score plot for MCI and HC subject groups (R2 = 0.924; Q2 = 0.792); (F) OPLS-DA score plot for AD and MCI subject groups (R2 = 0.971; Q2 = 0.691); QC = quality control.

of this metabolite did not differ between AD and MCI group. Glycolic acid, 3-hydroxypropanoic acid, and malic acid were lower in AD patients compared to MCI subjects, and malic acid was suggested to decrease with the progression of cognitive decline (from healthy controls through MCI subjects to AD patients). 2-Ketoisocaproic acid was decreased in both MCI and AD subjects in comparison to healthy individuals; however, the abundance of this compound could not be associated with the diagnosis of either AD or MCI, since there was no difference in the representation of this metabolite between these two groups.

Different organooxygen compounds, including glyceric acid, fructose and glucosaminic acid, showed lower levels in patients with AD, compared to both healthy controls and subjects with MCI. In the case of fructose, the abundance was also reduced in MCI subjects in comparison to healthy controls, with the abundance additionally decreasing towards AD diagnosis. The level of maltose and isomaltose was higher in AD patients and MCI subjects then in healthy control group. However, the abundance of these two disaccharides was lower in the subjects with AD, compared to individuals with MCI.

Significantly altered and identified metabolites, detected by LC-MS in both positive and negative ionization mode, are presented in Table 3. The list of metabolites, with the abundance significantly different in healthy controls compared to subjects diagnosed with AD or MCI, and/or significantly different in AD patients in comparison to individuals with MCI, was determined using the combination of multivariate and univariate statistics (Table 3). Most compounds detected by the LC-MS/MS approach, which were altered between the three groups of subjects included in this study, have been identified as different fatty acyls, glycerolipids and glycerophospholipids (Table 3). All of these compounds were decreased in AD patients and subjects with MCI compared to healthy controls. Other fatty acyls, glycerolipids and glycerophospholipids were significantly altered between subjects with AD or MCI and healthy individuals, however, their levels do not differentiate between AD and MCI group. Biliverdin was significantly increased, and bilirubin was significantly decreased, in subjects with cognitive impairments (AD and MCI group), compared to healthy controls (Table 3). Dehydroepiandrosterone sulfate (DHEAS), a multifunctional steroid produced mainly in the adrenal cortex, was less abundant in AD and MCI subjects in comparison to healthy individuals, but no difference was detected between subjects diagnosed with AD and the ones with MCI (Table 3).

Since subjects differed significantly in age, BMI and blood glucose concentration (Table 1), the parameters that could be associated with the abundance of specific metabolites, we wanted to rule out these variables as the main cause of the difference in the representation of individual metabolites between the examined groups. In order to test for the influence of age, BMI, and blood glucose levels on the abundance of different compounds in the plasma samples of the subjects, a correlation analysis was used, whilst controlling for the possible effect of diagnosis (Supplementary materials, Table S1). The partial correlation revealed no association between the level of individual metabolites and BMI or blood glucose concentration. In the case of age, the significant correlation was detected between age and the levels of pyroglutamic, glycolic, 3-hydroxypropanoic, malic and glucosaminic acid (Supplementary materials, Table S1). In order to determine the size of the effect of age on pyroglutamic, glycolic, 3-hydroxypropanoic, malic and glucosaminic acid levels, a multilinear regression model was performed (Supplementary materials, Table S2), with the concentration of individual metabolites as dependent variables, and with age and diagnosis as independent variables. The regression model demonstrated that age alone significantly affected only the concentration of malic acid. However, with the presence of diagnosis, as an additional independent variable, the predictive power of the model significantly increased (Supplementary materials, Table S2). Therefore, we can conclude that these multilinear regression

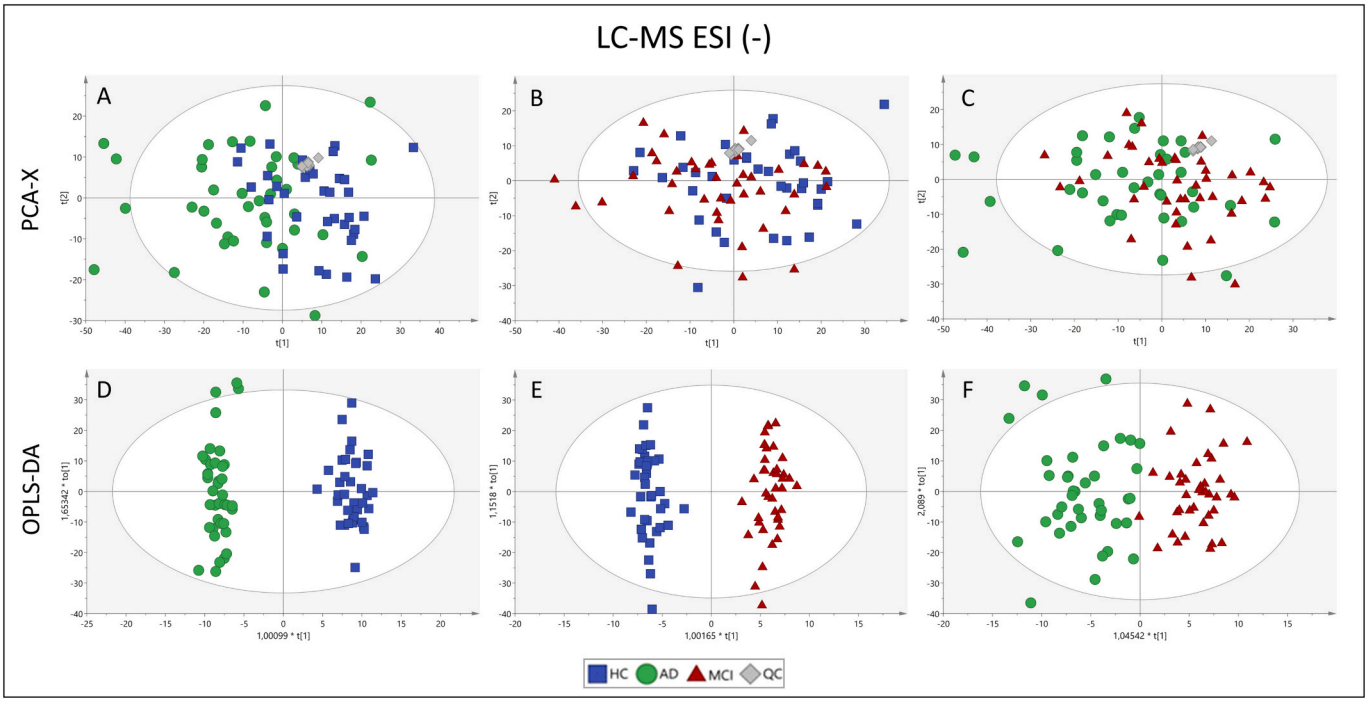

Fig. 5. PCA and OPLS-DA score plots of the untargeted metabolomics LC-MS ESI (−) analysis of plasma samples from healthy control individuals (HC), patients diagnosed with AD and subjects with MCI.
Plots were obtained using SIMCA-P+ software (version 15.0.2.5959, Umetrics, Umea, Sweden). The data matrix was pretreated using log-transformation and unit variance (UV) scaling method. (A) PCA score plot for AD and HC subject groups (R2X(cum) = 0.734); (B) PCA score plot for MCI and HC subject groups (R2X(cum) = 0.727); (C) PCA score plot for AD and MCI subject groups (R2X(cum) = 0.718); (D) OPLS-DA score plot for AD and HC subject groups (R2 = 0.969; Q2 = 0.809); (E) OPLS-DA score plot for MCI and HC subject groups (R2 = 0.966; Q2 = 0.776); (F) OPLS-DA score plot for AD and MCI subject groups (R2 = 0.656; Q2 = 0.307); QC = quality controls.

models demonstrated that the alternations in the level of pyroglutamic, glycolic, 3-hydroxypropanoic, malic and glucosaminic acid, are mainly due to diagnosis.

Our data revealed several significantly perturbed pathways, including aminoacyl-tRNA biosynthesis, glyoxylate and dicarboxylate metabolism, glycine, serine and threonine metabolism, porphyrin and butanoate metabolism, citrate cycle, glutathione metabolism, alanine, aspartate and glutamate metabolism, and arginine and proline metabolism (Supplementary materials, Fig. S1). A total of 15 distinct metabolites were identified from these pathways, including glycine, serine, methionine, valine, threonine, proline, glutamic acid, citric acid, malic acid, glyceric acid, biliverdin, bilirubin, acetoacetate, succinic acid, and hydroxyproline.

4. Discussion

The clinical diagnosis of AD is currently based on structured interviews with patients and their caregivers, accompanied by neuropsychological examinations combined with neuroimaging methods, all in order to rule out other potential causes of cognitive disfunction. However, the clinical diagnostic accuracy for AD is still not satisfying, especially during early stages of the disease when symptoms are similar to cognitive decline associated with normal aging (Porsteinsson et al., 2021). To approach this problem, we need biomarkers in clinical practice that would help the early and accurate detection of AD symptoms. For some time now, MCI has been considered as a prodromal phase of AD with the best predisposition for, more or less effective, pharmaceutical intervention. The diagnosis and treatment of AD is further complicated by the lack of reliable biomarkers that could help differentiate AD subjects from subjects in the prodromal stage of the disease. Blood-based biomarkers, unlike cerebrospinal fluid (CSF) biomarkers, have not yet entered the clinical practice, however, they have been widely explored due to their testing possibilities and fewer drawbacks compared to CSF. CSF sampling requires lumbar puncture which is an invasive method and not a routine clinical practice everywhere, while imaging methods are still very expensive and not widely available. Recently, convincing evidence has emerged supporting the use of plasma biomarkers (i.e., Aβ and phosphorylated tau) in clinical practice (Sabbagh et al., 2017). This step paves the way also for other blood-based biomarkers which could contribute to an earlier and/or more accurate diagnosis of AD. Metabolomic investigations give us the opportunity to find altered metabolites that could help better define the pathophysiology of the disease and search for circulating metabolites that might have the potential to aid AD diagnosis, evaluation of disease prognosis and the development of new therapeutic strategies. The aim of this study was to screen for metabolite signatures of AD pathology and to potentially identify new, easily accessible and cost-effective blood-based biomarkers for more accurate diagnosis of AD. Nevertheless, we have to bear in mind one of the main challenges in metabolomics studies, their limitation in associating metabolic changes in the periphery with those in the brain. Parallel targeted metabolomics study of both brain tissue and blood samples however identified a panel of sphingolipids whose concentrations in brain tissue were associated with severity of AD pathology and, in blood samples, with the progression of the disease, thus linking the alterations in metabolite signals in the brain tissue to those at the periphery (Varma et al., 2018).

In this study, the metabolomic profiling of the plasma samples obtained from AD patients, MCI subjects and healthy controls, was performed using the combined GC–MS and LC-MS approach. Using GC–MS approach we detected 88 compounds, among which significantly altered compounds belonged to the class of amino acids and their derivatives, fatty acids and organooxygen compounds. Using LC-MS ESI approach, in both positive and negative ionization mode, we identified 24 significantly altered metabolites from the classes of fatty acyls, glycerolipids,

Table 2
List of significantly altered compounds, detected by GC–MS analysis, between healthy controls, MCI subjects and AD patients.

Compound	RT	AD vs. HC			MCI vs. HC			AD vs. MCI		
		pBH	VIP	% Δ	pBH	VIP	% Δ	pBH	VIP	% Δ
Benzene and substituted derivatives										
Benzoic acid	9.55	NS	<1.00	6.6	1.32×10^{-4}	1.03	−27.2	4.46×10^{-4}	<1.00	46.4
Hippuric acid	16.91	NS	<1.00	3.8	7.99×10^{-5}	1.45	19.2	7.97×10^{-4}	1.53	−12.9
Carboxylic acids and derivatives										
Alanine	7.43	NS	<1.00	−17.7	NS	<1.00	4.4	3.26×10^{-2}	1.00	−21.1
Proline	8.59	8.86×10^{-3}	1.05	−30.0	NS	<1.00	−16.3	4.49×10^{-2}	1.08	−16.4
Valine	9.05	3.82×10^{-4}	1.00	−23.8	2.91×10^{-2}	1.03	−16.1	NS	<1.00	−9.1
Glycine	10.32	1.43×10^{-4}	1.30	−35.7	NS	<1.00	9.1	2.02×10^{-5}	1.63	−41.0
Succinic acid	10.42	6.16×10^{-12}	1.75	−45.3	2.50×10^{-6}	1.65	−30.8	1.42×10^{-3}	1.43	−20.9
Serine	11.04	7.32×10^{-3}	<1.00	−20.3	NS	<1.00	−0.9	3.26×10^{-2}	1.20	−19.6
Threonine	11.37	9.30×10^{-4}	1.03	−25.7	NS	<1.00	−2.8	1.89×10^{-3}	1.34	−23.5
2-Aminomalonic acid	12.48	NS	<1.00	−6.6	NS	<1.00	23.0	1.25×10^{-2}	1.35	−24.1
Methionine	13.11	NS	<1.00	−8.0	NS	<1.00	11.9	2.24×10^{-2}	1.02	−17.7
Pyroglutamic acid	13.14	3.24×10^{-3}	1.00	−21.4	NS	<1.00	5.2	3.49×10^{-4}	1.59	−25.3
4-Hydroxy-proline	13.18	NS	<1.00	−9.4	NS	<1.00	34.4	1.72×10^{-2}	1.06	−32.5
Glutamic acid	13.28	1.35×10^{-9}	1.73	−63.3	3.61×10^{-7}	1.72	−55.1	1.72×10^{-2}	<1.00	−18.3
Citric acid	16.52	1.14×10^{-2}	1.09	−10.9	4.91×10^{-2}	1.17	−4.0	NS	<1.00	−7.2
Fatty Acyls										
Nonanoic acid	11.08	NS	<1.00	−20.3	4.04×10^{-5}	1.36	−41.3	NS	<1.00	35.8
Citramalic acid	12.51	2.39×10^{-2}	<1.00	−3.8	NS	1.30	14.6	4.46×10^{-4}	1.08	−16.1
Hydroxy acids and derivatives										
Glycolic acid	7.03	9.75×10^{-8}	1.53	−26.8	NS	1.07	1.4	2.00×10^{-8}	1.99	−27.8
3-Hydroxypropanoic acid	8.02	6.59×10^{-7}	1.49	−25.5	NS	1.11	0.4	1.62×10^{-5}	1.83	−25.8
Malic acid	12.69	1.36×10^{-10}	1.71	−42.8	1.16×10^{-3}	1.50	−20.7	2.00×10^{-5}	1.66	−27.8
Keto acids and derivatives										
Acetoacetate	7.86	4.56×10^{-4}	1.14	75.1	6.65×10^{-4}	<1.00	76.4	NS	<1.00	−0.7
2-Ketoisocaproic acid	9.00	2.58×10^{-3}	1.11	−26.3	1.32×10^{-3}	1.38	−28.1	NS	<1.00	2.5
Organooxygen compounds										
Glyceric acid	10.63	1.14×10^{-12}	1.83	−40.5	NS	1.11	−8.6	2.00×10^{-8}	2.04	−34.9
Arabinose	14.78	NS	1.01	−3.1	NS	1.32	6.9	2.29×10^{-2}	1.19	−9.4
Fructose	17.05	1.03×10^{-4}	1.12	−38.5	4.91×10^{-2}	1.09	−32.9	1.50×10^{-2}	1.14	−8.4
Glucose	17.34	NS	1.03	−3.8	NS	1.18	1.0	3.02×10^{-2}	1.02	−4.8
Glucosaminic acid	18.37	9.05×10^{-6}	1.46	−26.7	NS	1.04	−0.4	2.00×10^{-5}	1.91	−26.4
Maltose	24.60	4.33×10^{-7}	1.55	36.5	1.86×10^{-9}	2.02	52.2	4.60×10^{-2}	1.11	−10.3
Isomaltose	25.55	1.00×10^{-2}	1.18	12.1	1.10×10^{-6}	1.85	24.8	1.10×10^{-2}	1.19	−10.2

%Δ, percentage of change; AD, Alzheimer's disease; HC, healthy controls; MCI, mild cognitive impairment; pBH, Benjamini-Hochberg adjusted p-value; RT, retention time in minutes; VIP, variable importance in the projection.

glycerophospholipids and sterol lipids.

One of the most consistent findings throughout AD metabolomic studies is the alteration of the amino acid metabolism. Amino acids are essential substrates and play an important role in regulation of many metabolic pathways, including aminoacyl-tRNA biosynthesis which is an essential process in protein synthesis (Wang et al., 2014a, 2014b, 2014c). Amino acids are precursors for various metabolites and lipids, important players in gene expression regulation and cell signaling (Wu, 2009). In the central nervous system, amino acids, including glutamic acid, γ-aminobutyric acid, aspartic acid, and glycine, are known to have an important role in neurotransmission (Dalangin et al., 2020). Many studies have reported altered amino acid levels in serum and brain of AD patients and AD animal models, but it remains unknown whether these changes really contribute to AD pathogenesis. The metabolic pathway analysis suggested that metabolic deregulations involved in AD pathogenesis, in both human AD patients and mouse models of AD, were significantly associated with associated with alanine, aspartate, purine, arginine, proline, and glutamate metabolism (Yin et al., 2023). Metabolomic studies which used the cerebrospinal fluid (CSF) samples from patients with AD have reported a diverse spectrum of altered metabolites, including arginine, valine, proline, serine, histidine, choline, creatine, and carnitine (Ibáñez et al., 2012). Additionally, perturbations in methionine, tryptophan, and tyrosine metabolic pathways have been observed, indicating their potential utility as viable biomarkers for diagnosis of AD (Griffin and Bradshaw, 2017; Kaddurah-Daouk et al., 2013). In present study, decreased levels of different amino acids and their derivates (proline, valine, glycine, succinic acid, serine, threonine, pyroglutamic, and glutamic acid) were observed in AD patients compared to both healthy controls and MCI group. Branched-chain amino acids (BCAA), namely valine, isoleucine and leucine, are essential amino acids involved in the protein synthesis and findings suggests that BCAA play a role in the brain functioning (Fernstrom, 2005). In accordance with our findings, lower plasma levels of valine were found to correlate with accelerated cognitive decline (González-Domínguez et al., 2015; Toledo et al., 2017). We have observed reduced levels of leucine metabolite, 2-ketoisocaproic acid, in both AD and MCI subjects compared to heathy controls. In contrast with these findings, Siddik and colleagues showed that levels of valine, isoleucine and leucine metabolites, as well as their keto- derivatives, such as ketoisocaproate, were significantly higher in AD patients in comparison to healthy controls (Siddik et al., 2022). Furthermore, alterations in glutamatergic neurotransmission have been associated with cognitive disorders, such as AD (Francis et al., 1993), ischemic brain damage (Bruno et al., 2001) and motor neuron disease (Gadea and López-Colomé, 2001). Glutamate

Table 3
Significantly altered metabolites, detected by LC-MS ESI, between patients diagnosed with AD, subjects with MCI, and healthy controls.

Compound	Mass	RT	ESI	AD vs. HC			MCI vs. HC			AD vs. MCI		
				pBH	VIP	% Δ	pBH	VIP	% Δ	pBH	VIP	% Δ
Fatty acyls												
9-HODE	296.2346	18.71	−	1.14×10^{-4}	1.30	−87.1%	6.69×10^{-6}	2.04	−96.2%	NS	0.62	240.4%
Eicosatetraenoic acid	304.2418	*27.83*	+	2.08×10^{-2}	0.66	−20.8%	6.80×10^{-3}	1.33	−30.7%	NS	0.93	14.2%
Dodecenoic acid	180.1493	29.91	+	6.35×10^{-3}	0.98	−32.4%	1.43×10^{-2}	1.39	−34.3%	NS	0.68	3.0%
Glycerolipids												
MG(16:0/0:0/0:0)	330.2748	28.23	+	2.77×10^{-4}	0.61	−29.1%	2.26×10^{-5}	1.67	−39.6%	NS	0.98	17.4%
MG(0:0/18:1/0:0)	356.2918	28.93	+	9.02×10^{-5}	1.14	−47.9%	4.90×10^{-6}	1.71	−53.6%	NS	0.70	12.1%
MG(18:2/0:0/0:0)	354.2747	25.74	+	1.04×10^{-3}	0.95	−40.0%	6.68×10^{-6}	1.81	−51.6%	NS	0.86	24.0%
Glycerophospholipids												
PC(O-12:0/2:0)	513.3052	14.45	−	7.00×10^{-5}	1.36	−46.8%	4.54×10^{-2}	1.19	−30.0%	6.89×10^{-2}	1.33	−24.0%
LysoPC(14:0/0:0)	513.3056	15.20	+	6.46×10^{-5}	1.37	−48.4%	4.23×10^{-2}	1.21	−31.4%	6.89×10^{-2}	1.38	−24.8%
LysoPC(15:0/0:0)	527.3211	16.42	−	6.46×10^{-5}	1.38	−40.6%	3.09×10^{-2}	1.20	−22.9%	NS	1.46	−22.9%
LysoPC(16:1/0:0)	539.3212	16.81	−	6.33×10^{-5}	1.44	−42.2%	4.80×10^{-2}	1.19	−23.8%	6.89×10^{-2}	1.58	−24.1%
PC(14:0/O-1:0)	481.3170	17.15	+	1.41×10^{-4}	1.14	−43.7%	2.96×10^{-2}	1.37	−28.4%	NS	1.26	−21.4%
PC(O-1:0/16:0)	509.3477	19.97	+	1.19×10^{-4}	1.17	−43.4%	2.47×10^{-2}	1.30	−29.7%	NS	1.18	−19.4%
LysoPC(18:1/0:0)	567.3523	20.72	−	1.78×10^{-6}	1.59	−52.9%	3.33×10^{-4}	1.77	−43.0%	NS	1.38	−17.4%
LysoPC(P-15:0/0:0)	465.3227	24.47	+	4.48×10^{-5}	1.14	−42.4%	3.49×10^{-3}	1.46	−31.5%	NS	1.31	−15.9%
PC(O-16:0/3:0)	537.3799	25.72	+	9.72×10^{-5}	1.27	−42.2%	1.61×10^{-2}	1.37	−27.8%	NS	1.29	−20.0%
PI(18:0/22:0)	958.6266	20.16	−	3.13×10^{-5}	1.36	−47.8%	5.01×10^{-3}	1.41	−33.3%	7.64×10^{-2}	1.01	−21.7%
LysoPE(18:1/0:0)	479.3002	20.51	−	1.01×10^{-5}	1.45	−58.9%	2.49×10^{-4}	1.73	−51.0%	NS	0.82	−16.2%
LysoPE(18:0/0:0)	463.3051	21.09	−	9.24×10^{-7}	1.66	−42.6%	5.83×10^{-5}	1.83	−33.7%	NS	1.17	−13.4%
Organoheterocyclic compounds												
Biliverdin	582.2455	13.26	+	3.40×10^{-4}	2.17	−61.5%	4.85×10^{-3}	1.15	−62.8%	NS	0.71	3.4%
Bilirubin	584.2641	34.16	+	3.55×10^{-4}	3.37	262.0%	4.93×10^{-3}	1.35	345.3%	NS	0.62	−18.7%
Sterol Lipids												
Dehydroepiandrosterone sulfate	368.1651	7.27	−	6.04×10^{-3}	0.91	−46.8%	9.43×10^{-3}	1.25	−52.0%	NS	0.17	10.7%

%Δ, percentage of change; AD, Alzheimer's disease; ESI, Electrospray ionization (the + sign indicates positive mode and the – sign negative ionization mode); HC, healthy controls; MCI, mild cognitive impairment; pBH, Benjamini-Hochberg adjusted *p*-value; RT, retention time in minutes; VIP, variable importance in the projection.

plays a prominent role in intermediary metabolism in all organs and tissues, linking carbohydrate and amino acid metabolism via tricarboxylic acid (TCA) cycle (Schousboe et al., 2014). Changes of glutamate and glutamine levels in AD may reflect altered neurotransmission and glutamate excitotoxicity, which involvement has been suggested in AD pathogenesis. Few studies reporting decreased levels of glutamate in AD and MCI subjects are in line with our results (Kim et al., 2019; Wang et al., 2014c). In addition, alternations in other key molecules of tricarboxylic acid (TCA) cycle and carbohydrate metabolism were observed in AD individuals through various metabolomic studies (Dong and Brewer, 2019; Van Der Velpen et al., 2019). In present study, a progressive reduction of key metabolites within the TCA cycle, namely succinic, citric, and malic acids, was observed starting from healthy controls, individuals with MCI, to the patients with AD. Consistent with our findings, similar metabolomic studies conducted on plasma samples have documented significant reductions in these metabolites, including 2-butanedioic and fumaric acid, in both AD and MCI subjects (Wang et al., 2014c). In a metabolomic study involving a mouse AD model, a significant decline in fumaric, citric, and malic acids was observed during aging (Wang et al., 2014a). Carbohydrate metabolism has been also altered in AD, with several studies reporting reduced glucose utilization, particularly in the hippocampus and posterior cingulate, during early stages of AD (Ferrari et al., 2019; Protas et al., 2013). This decline in glucose metabolism may contribute to the synaptic dysfunction and neuronal loss observed in AD (Sanabria-Diaz et al., 2013; Shivamurthy et al., 2015). Our results also indicated altered levels of metabolites that are directly or indirectly involved in the glycolytic pathway, including fructose, maltose, glyceric, and glucosaminic acid. The observed alterations in both metabolic pathways, glycolysis and TCA cycle, imply disrupted energy homeostasis in AD patients. These alterations seem to be reflected in both plasma and CSF samples of AD patients, suggesting their systemic origin (Van Der Velpen et al., 2019).

Benzoic acid is generally produced by gut microbial metabolic pathway ingestion of plant-based food that is rich with polyphenolic compounds (Ticinesi et al., 2023). Hippuric acid is a metabolite derived from the degradation of (poly)phenols and aromatic amino acids by gut microbiota, formed by the conjugation of benzoic acid with glycine and excreted in urine (Palau-Rodriguez et al., 2015). There are several metabolomic studies proposing hippuric acid as a biomarker of aging, since reduced levels of hippuric acid were found in the blood and urine samples of older participants with age-related diseases and cognitive impairment (Kameda et al., 2020; Saoi et al., 2019; Yilmaz et al., 2020). In the study conducted by Yilmaz and colleagues, excretion of hippuric acid was significantly reduced in MCI, but there was no difference between controls and patients with dementia (Yilmaz et al., 2020). In our study, we have detected decreased abundance of benzoic acid in MCI subjects in comparison to healthy controls, whereas the level of hippuric acid appeared to increase in individuals with MCI when compared to healthy controls and AD patients. Moreover, Trushina and colleagues identified several metabolites, including hippuric acid, that were elevated in the plasma of MCI subjects in comparison to controls (Trushina et al., 2013). Hence, the hippuric acid could be potentially considered as one of the metabolites for MCI detection.

Altered lipid metabolism and disturbance in the brain lipid levels are strongly associated with AD and age-associated cognitive decline (Ooi et al., 2021). Fatty acids, present at very high levels in neurons, are bioactive molecules, playing a vital role in the cell structure and signal transduction (Graber et al., 1994). In our study, we observed decreased levels of one of the metabolites of linoleic acid, 9-hydroxyoctadecadienoic acid (9-HODE), in AD patients in comparison to MCI subjects. In

study conducted by Cunnane and colleagues, linoleic acid was decreased in AD patients and MCI, when compared to healthy individuals (Cunnane et al., 2012). Lower levels of linoleic acid were associated with an increase of a pro-inflammatory metabolite, arachidonic acid (Fonteh et al., 2020). Many other fatty acids were also altered in AD, such as oleic, palmitic, and stearic acid, and, one of the most abundant polyunsaturated fatty acid (PUFA) in the brain, docosahexaenoic acid (DHA) (Belkouch et al., 2016; Cunnane et al., 2012; Fonteh et al., 2020; Snowden et al., 2017). An increasing number of studies have reported the potential association between alterations in fatty acid levels and AD (Devore et al., 2009). Moreover, it has been shown that elevated levels of free fatty acids induce amyloid deposition and tau hyperphosphorylation (Wilson and Binder, 1997). Various studies analyzed the levels of fatty acids in the brain, plasma or serum of AD patients, but with contradictory results (Cunnane et al., 2012; Fraser et al., 2010; Wang et al., 2012). The alterations of fatty acid metabolism in the peripheral blood of AD patients could reflect the abnormal fatty acids metabolism in the brain tissue, associated with altered synaptic function and neuroinflammation, due to the ability of fatty acids to pass freely through the blood–brain barrier. Therefore, the monitoring of abnormal fatty acids metabolism at the periphery could be of great significance in early diagnosis of AD.

Glycerophospholipids are polar lipids, with main role in the transportation, metabolic reactions, development, apoptosis and signal induction and transmission (Akyol et al., 2021). Glycerophospholipids are divided in the subgroups of phosphatidylcholines (PC), phosphatidylserines (PS), phosphatidylethanolamines (PE), and phosphatidylinositols (PI). Our results showed significantly decreased levels of different PCs, PEs and PI(18:0/22:0) in AD patients and MCI subjects compared to the healthy controls. Out of all detected glycerophospholipids, PC(O-12:0/2:0), LysoPC(14:0/0:0), LysoPC(16:1/0:0), and PI(18:0/22:0) could possibly have prognostic value, since their levels are decreasing from healthy controls to MCI subjects and finally to AD patients. A decrease in PCs and lysoPCs levels in patients with AD has been previously reported (González-Domínguez et al., 2015; Mapstone et al., 2014; Whiley et al., 2014). The reduced levels of PCs might be linked with the aberrant activity of phospoholipase A2 (PLA2), enzyme involved in cleavage of fatty acids, producing free fatty acids and LysoPCs (Burke and Dennis, 2009). The activity of this enzyme appears to be increased in the presence of β-amyloid peptide, the major component of the amyloid plaques and one of the main hallmarks of AD (Hicks et al., 2008). In our study we observed altered levels of LysoPCs in plasma of AD patients, which is in line with other studies focused on plasma (González-Domínguez et al., 2014; Li et al., 2010) and CSF (Mulder et al., 2003) samples, while Grimm et al. reported partial increase of LysoPCs levels in postmortem AD brains (Grimm et al., 2011). Reason for these discrepancies is that LysoPCs are not only intermediates in glycerophospholipid metabolism, but they are also involved in the multiple neuronal pathways (Frisardi et al., 2011).

Glycerolipids can be categorized into triacylglycerols (TG), monoacylglycerol (MG), and diacylglycerol (DAG), based on the number of acyl groups in the structure. It appears that TG levels were not altered in the plasma of AD patients (Proitsi et al., 2017), however, levels of both MG and DG were elevated in both prefrontal cortex and plasma of AD and MCI subjects, suggesting change in the glycerolipid metabolism as an early event in AD (Chan et al., 2012; Wood et al., 2015b). In addition, one study demonstrated increased MG and DG levels in the gray matter of MCI and AD patients, indicating that these changes may play a role in the development of MCI, as well as transition from MCI to AD (Wood et al., 2015a). However, we observed lower levels of MG(0:0/18:1/0:0) in AD and MCI in comparison to control subjects, and no differences were detected between AD and MCI group.

Steroid lipids are important components in the pathophysiology of AD and their role has been studied intensively, but metabolomic data are limited. Dehydroepiandrosterone (DHEA) and its sulphate (DHEAS) are neurosteroids, secreted mainly by the adrenal cortex, with role in a wide variety of physiological systems, and with the effect on the brain (Kroboth et al., 1999), immune system (Chen and Parker, 2004), somatic growth and development (Arquitt et al., 1991). Levels of these steroids decrease with aging, suggesting association with a decrease in cognitive function, as well as the increased rates of neuronal degeneration and dysfunction that occur during aging (Berr et al., 1996). In our study, DHEAS was found to be less abundant in AD and MCI subjects compared to healthy individuals, but no differences were detected between subjects diagnosed with AD or MCI. Many studies confirmed reduction in levels of DHEAS in the plasma of patients suffering from AD (Cho et al., 2006; Genedani et al., 2004; Kalecký et al., 2022). However, there is inconsistence between circulating levels of steroid hormones and those reported in the brain, since several studies reported elevated levels in AD brain tissue (Brown et al., 2003; Marx et al., 2006). It has been proposed that increase in DHEA levels in the brain represents a response to an increased oxidative stress induced by the presence of amyloid peptides in AD (Cardounel et al., 1999). It is hypothesized that DHEA is sequestered away in the brain of AD patients, resulting in the further decrease of DHEA levels in circulation (Aldred and Mecocci, 2010). Oxidative stress contributes to the AD pathophysiology by causing mitochondrial dysfunction, accumulation of reactive oxygen species (ROS) and consequently upregulation of p-tau and Aβ synthesis (Cassidy et al., 2020; Konjevod et al., 2021). One of the antioxidants that acts as scavenger of ROS in brain, bilirubin, was found to be decreased in the plasma of patients with AD and MCI, while biliverdin, used for conversion to bilirubin, was significantly increased. However, metabolomic study of Trushina et al. reported reduction in the plasma and CSF levels of both bilirubin and biliverdin in AD individuals in comparison to MCI and controls (Trushina et al., 2013). Other studies also reported lower levels of antioxidants in plasma of AD patients, including bilirubin, supporting the hypothesis that oxidative injury may have important role in the pathogenesis of AD (Di Domenico et al., 2012; Kim et al., 2006).

The main limitation of this study is its cross-sectional design since the longitudinal follow-up would allow us to identify those MCI patients and healthy controls who will potentially develop dementia over time. Another limitation of the study is the difference in age, BMI and blood glucose level between subject groups. The study included only elderly population (age $\geq$ 65 years) in order do minimalize the age-dependent metabolome changes. We also used correlation analysis and multilinear regression model in order to rule out age, BMI and blood glucose level as the main cause of the difference in the representation of individual metabolites between the examined groups. However, despite additional analyzes showing that diagnosis is the main parameter that contributes to the difference between the compared groups, we cannot definitively claim that age, BMI and blood glucose level have no influence on the abundance of investigated metabolites. Strengths of the study are in the inclusion of ethnically homogenous groups and adequate sample size, along with needed statistical power. However, further studies are needed to validate our findings. In order to support these results, multicenter clinical validation trials and metabolomics-based longitudinal studies with larger sample sizes will be crucial.

5. Conclusion

In this study, we applied the untargeted metabolomic approach to investigate the changes in biochemical pathways related to AD pathology. The multiplatform metabolomic profiling of the plasma samples from AD patients, MCI subjects and healthy controls revealed significantly altered levels of compounds belonging to the class of amino acids and their derivatives, fatty acids, organooxygen compounds, fatty acyls, glycerolipids, glycerophospholipids and sterol lipids. The results of this study indicate disturbed metabolism of lipids and amino acids and an imbalance of metabolites involved in the energy metabolism in patients diagnosed with AD, compared to the healthy controls and MCI subjects, suggesting potential, easily accessible, diagnostic and prognostic metabolomic biomarkers of AD.

Informed consent statement

Informed consent was obtained from all subjects involved in this study.

Ethical statement

The study was approved by the Ethics Committee of University Psychiatric Hospital Vrapce, Zagreb, Croatia (approval code 23–605/3–18; March 23, 2018) and carried out in line with the Helsinki Declaration (World Medical Association, 2013). All subjects have signed informed consent prior to participating in the study and the study procedures were explained in details to the participants and/or their caregivers.

Funding

This work was supported by the by the offset project founded by Patria [grant number CRO_A-00033]; and by the Croatian Science Foundation research [IP-2019-04-6100].

CRediT authorship contribution statement

Tina Milos: Formal analysis, Investigation, Visualization, Writing – original draft. **David Rojo:** Data curation, Formal analysis, Investigation, Methodology, Supervision, Writing – review & editing. **Gordana Nedic Erjavec:** Methodology. **Marcela Konjevod:** Methodology. **Lucija Tudor:** Visualization. **Barbara Vuic:** Writing – original draft. **Dubravka Svob Strac:** Funding acquisition, Writing – review & editing. **Suzana Uzun:** Resources. **Ninoslav Mimica:** Resources. **Oliver Kozumplik:** Resources. **Coral Barbas:** Project administration, Resources, Supervision, Writing – review & editing. **Neven Zarkovic:** Funding acquisition, Project administration, Resources, Supervision, Writing – review & editing. **Nela Pivac:** Resources, Writing – review & editing. **Matea Nikolac Perkovic:** Conceptualization, Data curation, Formal analysis, Investigation, Methodology, Supervision, Visualization, Writing – original draft, Writing – review & editing.

Declaration of Competing Interest

The authors declare the following financial interests/personal relationships which may be considered as potential competing interests.

Dubravka Svob Strac reports financial support was provided by Croatian Science Foundation. Neven Zarkovic and Coral Barbas report financial support provided by Patria Oyj.

Data availability

All the data reported are available on request from the corresponding author.

Acknowledgements

The author would like to acknowledge the contribution of Croatian Science Foundation's "Young Researchers' Career Development Project" [grant number DOK-2021-02-2553 and DOK-2020-01-3622] since it was requested by Croatian Science Foundation.

Appendix A. Supplementary data

Supplementary data to this article can be found online at https://doi.org/10.1016/j.pnpbp.2023.110830.

References

Akyol, S., Ugur, Z., Yilmaz, A., Ustun, I., Gorti, S.K.K., Oh, K., McGuinness, B., Passmore, P., Kehoe, P.G., Maddens, M.E., Green, B.D., Graham, S.F., 2021. Lipid profiling of Alzheimer's disease brain highlights enrichment in glycerol(phospho) lipid, and sphingolipid metabolism. Cells 10. https://doi.org/10.3390/cells10102591.

Albert, M.S., DeKosky, S.T., Dickson, D., Dubois, B., Feldman, H.H., Fox, N.C., Gamst, A., Holtzman, D.M., Jagust, W.J., Petersen, R.C., Snyder, P.J., Carrillo, M.C., Thies, B., Phelps, C.H., 2011. The diagnosis of mild cognitive impairment due to Alzheimer's disease: recommendations from the National Institute on Aging-Alzheimer's Association workgroups on diagnostic guidelines for Alzheimer's disease. Alzheimers Dement. 7, 270–279. https://doi.org/10.1016/j.jalz.2011.03.008.

Aldred, S., Mecocci, P., 2010. Decreased dehydroepiandrosterone (DHEA) and dehydroepiandrosterone sulfate (DHEAS) concentrations in plasma of Alzheimer's disease (AD) patients. Arch. Gerontol. Geriatr. 51, e16–e18. https://doi.org/10.1016/j.archger.2009.07.001.

APA, 2013. Diagnostic and Statistical Manual of Mental Disorders, 5th ed. Arlington, VA.

Arevalo-Rodriguez, I., Smailagic, N., Roqué, I., Figuls, M., Ciapponi, A., Sanchez-Perez, E., Giannakou, A., Pedraza, O.L., Bonfill Cosp, X., Cullum, S., 2015. Mini-mental state examination (MMSE) for the detection of Alzheimer's disease and other dementias in people with mild cognitive impairment (MCI). Cochrane Database Syst. Rev. 2015 https://doi.org/10.1002/14651858.CD010783.pub2. CD010783.

Armitage, E.G., Godzien, J., Alonso-Herranz, V., López-Gonzálvez, Á., Barbas, C., 2015. Missing value imputation strategies for metabolomics data. Electrophoresis. 36, 3050–3060. https://doi.org/10.1002/elps.201500352 (PMID: 26376450).

Arquitt, A.B., Stoecker, B.J., Hermann, J.S., Winterfeldt, E.A., 1991. Dehydroepiandrosterone sulfate, cholesterol, hemoglobin, and anthropometric measures related to growth in male adolescents. J. Am. Diet. Assoc. 91, 575–579.

Belkouch, M., Hachem, M., Elgot, A., Lo Van, A., Picq, M., Guichardant, M., Lagarde, M., Bernoud-Hubac, N., 2016. The pleiotropic effects of omega-3 docosahexaenoic acid on the hallmarks of Alzheimer's disease. J. Nutr. Biochem. 38, 1–11. https://doi.org/10.1016/j.jnutbio.2016.03.002.

Berr, C., Lafont, S., Debuire, B., Dartigues, J.F., Baulieu, E.E., 1996. Relationships of dehydroepiandrosterone sulfate in the elderly with functional, psychological, and mental status, and short-term mortality: a French community-based study. Proc. Natl. Acad. Sci. U. S. A. 93, 13410–13415. https://doi.org/10.1073/pnas.93.23.13410.

Brown, R.C., Han, Z., Cascio, C., Papadopoulos, V., 2003. Oxidative stress-mediated DHEA formation in Alzheimer's disease pathology. Neurobiol. Aging 24, 57–65. https://doi.org/10.1016/s0197-4580(02)00048-9.

Bruno, V., Battaglia, G., Copani, A., D'Onofrio, M., Di Iorio, P., De Blasi, A., Melchiorri, D., Flor, P.J., Nicoletti, F., 2001. Metabotropic glutamate receptor subtypes as targets for neuroprotective drugs. J. Cereb. Blood Flow Metab. 21, 1013–1033. https://doi.org/10.1097/00004647-200109000-00001.

Burke, J.E., Dennis, E.A., 2009. Phospholipase A2 biochemistry. Cardiovasc. Drugs Ther. 23, 49–59. https://doi.org/10.1007/s10557-008-6132-9.

Cardounel, A., Regelson, W., Kalimi, M., 1999. Dehydroepiandrosterone protects hippocampal neurons against neurotoxin-induced cell death: Mechanism of action. In: Proc. Soc. Exp. Biol. Med. Soc. Exp. Biol. Med. (New York, N.Y.), vol. 222, pp. 145–149. https://doi.org/10.1046/j.1525-1373.1999.d01-124.x.

Cassidy, L., Fernandez, F., Johnson, J.B., Naiker, M., Owoola, A.G., Broszczak, D.A., 2020. Oxidative stress in alzheimer's disease: a review on emergent natural polyphenolic therapeutics. Complement. Ther. Med. 49, 102294 https://doi.org/10.1016/j.ctim.2019.102294.

Chan, R.B., Oliveira, T.G., Cortes, E.P., Honig, L.S., Duff, K.E., Small, S.A., Wenk, M.R., Shui, G., Di Paolo, G., 2012. Comparative lipidomic analysis of mouse and human brain with Alzheimer disease. J. Biol. Chem. 287, 2678–2688. https://doi.org/10.1074/jbc.M111.274142.

Chang, C.-C., Lin, C.-J., 2011. LIBSVM: a library for support vector machines. ACM Trans. Intell. Syst. Technol. 2, 1–27. https://doi.org/10.1145/1961189.1961199.

Chen, C.C.G., Parker, C.R.J., 2004. Adrenal androgens and the immune system. Semin. Reprod. Med. 22, 369–377. https://doi.org/10.1055/s-2004-861553.

Cho, S.-H., Jung, B.H., Lee, W.-Y., Chung, B.C., 2006. Rapid column-switching liquid chromatography/mass spectrometric assay for DHEA-sulfate in the plasma of patients with Alzheimer's disease. Biomed. Chromatogr. 20, 1093–1097. https://doi.org/10.1002/bmc.647.

Cunnane, S.C., Schneider, J.A., Tangney, C., Tremblay-Mercier, J., Fortier, M., Bennett, D.A., Morris, M.C., 2012. Plasma and brain fatty acid profiles in mild cognitive impairment and Alzheimer's disease. J. Alzheimers Dis. 29, 691–697. https://doi.org/10.3233/JAD-2012-110629.

Dalangin, R., Kim, A., Campbell, R.E., 2020. The role of amino acids in neurotransmission and fluorescent tools for their detection. Int. J. Mol. Sci. 21, 6197. https://doi.org/10.3390/ijms21176197.

De Livera, A.M., Dias, D.A., De Souza, D., Rupasinghe, T., Pyke, J., Tull, D., Roessner, U., McConville, M., Speed, T.P., 2012. Normalizing and integrating metabolomics data. Anal. Chem. 84, 10768–10776. https://doi.org/10.1021/ac302748b.

Devore, E.E., Grodstein, F., van Rooij, F.J.A., Hofman, A., Rosner, B., Stampfer, M.J., Witteman, J.C.M., Breteler, M.M.B., 2009. Dietary intake of fish and omega-3 fatty acids in relation to long-term dementia risk. Am. J. Clin. Nutr. 90, 170–176. https://doi.org/10.3945/ajcn.2008.27037.

Di Domenico, F., Baroneb, E., Mancuso, C., Perluigi, M., Cocciolo, A., Mecocci, P., Butterfield, D.A., Coccia, R., 2012. HO-1/BVR-A system analysis in plasma from probable Alzheimer's disease and mild cognitive impairment subjects: a potential biochemical marker for the prediction of the disease. J. Alzheimers Dis. 32, 277–289. https://doi.org/10.3233/JAD-2012-121045.

Dong, Y., Brewer, G.J., 2019. Global metabolic shifts in age and Alzheimer's disease mouse brains pivot at NAD+/NADH redox sites. J. Alzheimers Dis. 71, 119–140. https://doi.org/10.3233/JAD-190408.
Fahy, E., Sud, M., Cotter, D., Subramaniam, S., 2007. LIPID MAPS online tools for lipid research. Nucleic Acids Res. 35, W606–W612. https://doi.org/10.1093/nar/gkm324.
Faul, F., Erdfelder, E., Lang, A.-G., Buchner, A., 2007. G*power 3: a flexible statistical power analysis program for the social, behavioral, and biomedical sciences. Behav. Res. Methods 39, 175–191. https://doi.org/10.3758/BF03193146.
Fernstrom, J.D., 2005. Branched-chain amino acids and brain function. J. Nutr. 135, 1539S–1546S. https://doi.org/10.1093/jn/135.6.1539S.
Ferrari, B.L., de Neto, G.C.C., Nucci, M.P., Mamani, J.B., Lacerda, S.S., Felício, A.C., Amaro, E.J., Gamarra, L.F., 2019. The accuracy of hippocampal volumetry and glucose metabolism for the diagnosis of patients with suspected Alzheimer's disease, using automatic quantitative clinical tools. Medicine (Baltimore) 98, e17824. https://doi.org/10.1097/MD.0000000000017824.
Fonteh, A.N., Cipolla, M., Chiang, A.J., Edminster, S.P., Arakaki, X., Harrington, M.G., 2020. Polyunsaturated fatty acid composition of cerebrospinal fluid fractions shows their contribution to cognitive resilience of a pre-symptomatic Alzheimer's disease cohort. Front. Physiol. 11, 83. https://doi.org/10.3389/fphys.2020.00083.
Francis, P.T., Sims, N.R., Procter, A.W., Bowen, D.M., 1993. Cortical pyramidal Neurone loss may cause glutamatergic Hypoactivity and cognitive impairment in Alzheimer's disease: investigative and therapeutic perspectives. J. Neurochem. 60, 1589–1604. https://doi.org/10.1111/j.1471-4159.1993.tb13381.x.
Fraser, T., Tayler, H., Love, S., 2010. Fatty acid composition of frontal, temporal and parietal neocortex in the Normal human brain and in Alzheimer's disease. Neurochem. Res. 35, 503–513. https://doi.org/10.1007/s11064-009-0087-5.
Frisardi, V., Panza, F., Seripa, D., Farooqui, T., Farooqui, A.A., 2011. Glycerophospholipids and glycerophospholipid-derived lipid mediators: a complex meshwork in Alzheimer's disease pathology. Prog. Lipid Res. 50, 313–330. https://doi.org/10.1016/j.plipres.2011.06.001.
Gadea, A., López-Colomé, A.M., 2001. Glial transporters for glutamate, glycine, and GABA: II. GABA transporters. J. Neurosci. Res. 63, 461–468. https://doi.org/10.1002/jnr.1040.
Genedani, S., Rasio, G., Cortelli, P., Antonelli, F., Guidolin, D., Galantucci, M., Fuxe, K., Agnati, L.F., 2004. Studies on homocysteine and dehydroepiandrosterone sulphate plasma levels in Alzheimer's disease patients and in Parkinson's disease patients. Neurotox. Res. 6, 327–332. https://doi.org/10.1007/BF03033443.
Gil de la Fuente, A., Godzien, J., Fernández López, M., Rupérez, F.J., Barbas, C., Otero, A., 2018. Knowledge-based metabolite annotation tool: CEU mass mediator. J. Pharm. Biomed. Anal. 154, 138–149. https://doi.org/10.1016/j.jpba.2018.02.046.
Godzien, J., Alonso-Herranz, V., Barbas, C., Armitage, E.G., 2015. Controlling the quality of metabolomics data: new strategies to get the best out of the QC sample. Metabolomics 11, 518–528. https://doi.org/10.1007/s11306-014-0712-4.
González-Domínguez, R., García-Barrera, T., Gómez-Ariza, J.L., 2014. Combination of metabolomic and phospholipid-profiling approaches for the study of Alzheimer's disease. J. Proteome 104, 37–47. https://doi.org/10.1016/j.jprot.2014.01.014.
González-Domínguez, R., García-Barrera, T., Gómez-Ariza, J.L., 2015. Metabolite profiling for the identification of altered metabolic pathways in Alzheimer's disease. J. Pharm. Biomed. Anal. 107, 75–81. https://doi.org/10.1016/j.jpba.2014.10.010.
Graber, R., Sumida, C., Nunez, E.A., 1994. Fatty acids and cell signal transduction. J. Lipid Mediat. Cell Signal. 9, 91–116.
Griffin, J.W.D., Bradshaw, P.C., 2017. Amino acid catabolism in Alzheimer's disease brain: friend or foe? Oxidative Med. Cell. Longev. 2017, 5472792. https://doi.org/10.1155/2017/5472792.
Grimm, M.O.W., Grösgen, S., Riemenschneider, M., Tanila, H., Grimm, H.S., Hartmann, T., 2011. From brain to food: analysis of phosphatidylcholins, lyso-phosphatidylcholins and phosphatidylcholin-plasmalogens derivates in Alzheimer's disease human post mortem brains and mice model via mass spectrometry. J. Chromatogr. A 1218, 7713–7722. https://doi.org/10.1016/j.chroma.2011.07.073.
Gromski, P.S., Xu, Y., Hollywood, K.A., Turner, M.L., Goodacre, R., 2015. The influence of scaling metabolomics data on model classification accuracy. Metabolomics 11, 684–695. https://doi.org/10.1007/s11306-014-0738-7.
Hicks, J.B., Lai, Y., Sheng, W., Yang, X., Zhu, D., Sun, G.Y., Lee, J.C.-M., 2008. Amyloid-beta peptide induces temporal membrane biphasic changes in astrocytes through cytosolic phospholipase A2. Biochim. Biophys. Acta 1778, 2512–2519. https://doi.org/10.1016/j.bbamem.2008.07.027.
Huo, Z., Yu, L., Yang, J., Zhu, Y., Bennett, D.A., Zhao, J., 2020. Brain and blood metabolome for Alzheimer's dementia: findings from a targeted metabolomics analysis. Neurobiol. Aging 86, 123–133. https://doi.org/10.1016/j.neurobiolaging.2019.10.014.
Ibáñez, C., Simó, C., Martín-Álvarez, P.J., Kivipelto, M., Winblad, B., Cedazo-Mínguez, A., Cifuentes, A., 2012. Toward a predictive model of Alzheimer's disease progression using capillary electrophoresis-mass spectrometry metabolomics. Anal. Chem. 84, 8532–8540. https://doi.org/10.1021/ac301243k.
Kaddurah-Daouk, R., Zhu, H., Sharma, S., Bogdanov, M., Rozen, S.G., Matson, W., Oki, N. O., Motsinger-Reif, A.A., Churchill, E., Lei, Z., Appleby, D., Kling, M.A., Trojanowski, J.Q., Doraiswamy, P.M., Arnold, S.E., Network, P.R., 2013. Alterations in metabolic pathways and networks in Alzheimer's disease. Transl. Psychiatry 3, e244. https://doi.org/10.1038/tp.2013.18.
Kaleckỳ, K., German, D.C., Montillo, A.A., Bottiglieri, T., 2022. Targeted Metabolomic analysis in Alzheimer's disease plasma and brain tissue in non-Hispanic whites. J. Alzheimers Dis. 86, 1875–1895. https://doi.org/10.3233/JAD-215448.
Kameda, M., Teruya, T., Yanagida, M., Kondoh, H., 2020. Frailty markers comprise blood metabolites involved in antioxidation, cognition, and mobility. Proc. Natl. Acad. Sci. U. S. A. 117, 9483–9489. https://doi.org/10.1073/pnas.1920795117.
Kanehisa, M., Goto, S., 2000. KEGG: Kyoto encyclopedia of genes and genomes. Nucleic Acids Res. 28, 27–30. https://doi.org/10.1093/nar/28.1.27.
Kim, T.S., Pae, C.U., Yoon, S.J., Jang, W.Y., Lee, N.J., Kim, J.J., Lee, S.J., Lee, C., Paik, I. H., Lee, C.U., 2006. Decreased plasma antioxidants in patients with Alzheimer's disease. Int. J. Geriatr. Psychiatry 21, 344–348. https://doi.org/10.1002/gps.1469.
Kim, Y.H., Shim, H.S., Kim, K.H., Junghee, L., Chung, B.C., Kowall, N.W., Ryu, H., Jeongae, L., 2019. Metabolomic analysis identifies alterations of amino acid metabolome signatures in the postmortem brain of Alzheimer's disease. Exp. Neurobiol. 28, 376–389. https://doi.org/10.5607/en.2019.28.3.376.
Konjevod, M., Nikolac Perkovic, M., Sáiz, J., Svob Strac, D., Barbas, B., Rojo, D., 2021. Metabolomics analysis of microbiota-gut-brain axis in neurodegenerative and psychiatric diseases. J. Pharm. Biomed. Anal. 194, 113681 https://doi.org/10.1016/j.jpba.2020.113681.
Kroboth, P.D., Salek, F.S., Pittenger, A.L., Fabian, T.J., Frye, R.F., 1999. DHEA and DHEA-S: a review. J. Clin. Pharmacol. 39, 327–348. https://doi.org/10.1177/00912709922007903.
Kuligowski, J., Sánchez-Illana, Á., Sanjuán-Herráez, D., Vento, M., Quintás, G., 2015. Intra-batch effect correction in liquid chromatography-mass spectrometry using quality control samples and support vector regression (QC-SVRC). Analyst 140, 7810–7817. https://doi.org/10.1039/C5AN01638J.
Li, N., Liu, W., Li, W., Li, S., Chen, X., Bi, K., He, P., 2010. Plasma metabolic profiling of Alzheimer's disease by liquid chromatography/mass spectrometry. Clin. Biochem. 43, 992–997. https://doi.org/10.1016/j.clinbiochem.2010.04.072.
Mapstone, M., Cheema, A.K., Fiandaca, M.S., Zhong, X., Mhyre, T.R., MacArthur, L.H., Hall, W.J., Fisher, S.G., Peterson, D.R., Haley, J.M., Nazar, M.D., Rich, S.A., Berlau, D.J., Peltz, C.B., Tan, M.T., Kawas, C.H., Federoff, H.J., 2014. Plasma phospholipids identify antecedent memory impairment in older adults. Nat. Med. 20, 415–418. https://doi.org/10.1038/nm.3466.
Marx, C.E., Trost, W.T., Shampine, L.J., Stevens, R.D., Hulette, C.M., Steffens, D.C., Ervin, J.F., Butterfield, M.I., Blazer, D.G., Massing, M.W., Lieberman, J.A., 2006. The neurosteroid allopregnanolone is reduced in prefrontal cortex in Alzheimer's disease. Biol. Psychiatry 60, 1287–1294. https://doi.org/10.1016/j.biopsych.2006.06.017.
McKhann, G.M., Knopman, D.S., Chertkow, H., Hyman, B.T., Jack, C.R.J., Kawas, C.H., Klunk, W.E., Koroshetz, W.J., Manly, J.J., Mayeux, R., Mohs, R.C., Morris, J.C., Rossor, M.N., Scheltens, P., Carrillo, M.C., Thies, B., Weintraub, S., Phelps, C.H., 2011. The diagnosis of dementia due to Alzheimer's disease: recommendations from the National Institute on Aging-Alzheimer's Association workgroups on diagnostic guidelines for Alzheimer's disease. Alzheimers Dement. 7, 263–269. https://doi.org/10.1016/j.jalz.2011.03.005.
Mulder, C., Wahlund, L.-O., Teerlink, T., Blomberg, M., Veerhuis, R., van Kamp, G.J., Scheltens, P., Scheffer, P.G., 2003. Decreased lysophosphatidylcholine/phosphatidylcholine ratio in cerebrospinal fluid in Alzheimer's disease. J. Neural Transm. 110, 949–955. https://doi.org/10.1007/s00702-003-0007-9.
Ooi, K.-L.M., Vacy, K., Boon, W.C., 2021. Fatty acids and beyond: age and Alzheimer's disease related changes in lipids reveal the neuro-nutraceutical potential of lipids in cognition. Neurochem. Int. 149, 105143 https://doi.org/10.1016/j.neuint.2021.105143.
Palau-Rodriguez, M., Tulipani, S., Isabel Queipo-Ortuño, M., Urpi-Sarda, M., Tinahones, F.J., Andres-Lacueva, C., 2015. Metabolomic insights into the intricate gut microbial-host interaction in the development of obesity and type 2 diabetes. Front. Microbiol. 6, 1151. https://doi.org/10.3389/fmicb.2015.01151.
Pang, Z., Chong, J., Zhou, G., de Lima Morais, D.A., Chang, L., Barrette, M., Gauthier, C., Jacques, P.-É., Li, S., Xia, J., 2021. MetaboAnalyst 5.0: narrowing the gap between raw spectra and functional insights. Nucleic Acids Res. 49, W388–W396. https://doi.org/10.1093/nar/gkab382.
Petersen, R.C., Lopez, O., Armstrong, M.J., Getchius, T.S.D., Ganguli, M., Gloss, D., Gronseth, G.S., Marson, D., Pringsheim, T., Day, G.S., Sager, M., Stevens, J., Rae-Grant, A., 2018. Practice guideline update summary: mild cognitive impairment: report of the guideline development, dissemination, and implementation Subcommittee of the American Academy of neurology. Neurology 90, 126–135. https://doi.org/10.1212/WNL.0000000000004826.
Porsteinsson, A.P., Isaacson, R.S., Knox, S., Sabbagh, M.N., Rubino, I., 2021. Diagnosis of early Alzheimer's disease: Clinical practice in 2021. J. Prev. Alzheimers Dis. 8 https://doi.org/10.14283/jpad.2021.23.
Proitsi, P., Kim, M., Whiley, L., Simmons, A., Sattlecker, M., Velayudhan, L., Lupton, M. K., Soininen, H., Kloszewska, I., Mecocci, P., Tsolaki, M., Vellas, B., Lovestone, S., Powell, J.F., Dobson, R.J.B., Legido-Quigley, C., 2017. Association of blood lipids with Alzheimer's disease: a comprehensive lipidomics analysis. Alzheimers Dement. 13, 140–151. https://doi.org/10.1016/j.jalz.2016.08.003.
Protas, H.D., Chen, K., Langbaum, J.B.S., Fleisher, A.S., Alexander, G.E., Lee, W., Bandy, D., de Leon, M.J., Mosconi, L., Buckley, S., Truran-Sacrey, D., Schuff, N., Weiner, M.W., Caselli, R.J., Reiman, E.M., 2013. Posterior cingulate glucose metabolism, hippocampal glucose metabolism, and hippocampal volume in cognitively normal, late-middle-aged persons at 3 levels of genetic risk for Alzheimer disease. JAMA Neurol. 70, 320–325. https://doi.org/10.1001/2013.jamaneurol.286.
Rani, P., Krishnan, S., Rani Cathrine, C., 2017. Study on analysis of peripheral biomarkers for Alzheimer's disease diagnosis. Front. Neurol. 8, 328. https://doi.org/10.3389/fneur.2017.00328.
Sabbagh, M.N., Lue, L.F., Fayard, D., Shi, J., 2017. Increasing precision of clinical diagnosis of Alzheimer's disease using a combined algorithm incorporating clinical

and novel biomarker data. Neurol. Ther. 6, 83–95. https://doi.org/10.1007/s40120-017-0069-5.
Sanabria-Diaz, G., Martínez-Montes, E., Melie-Garcia, L., 2013. Glucose metabolism during resting state reveals abnormal brain networks organization in the Alzheimer's disease and mild cognitive impairment. PLoS One 8, e68860. https://doi.org/10.1371/journal.pone.0068860.
Saoi, M., Li, A., McGlory, C., Stokes, T., von Allmen, M.T., Phillips, S.M., Britz-McKibbin, P., 2019. Metabolic perturbations from step reduction in older persons at risk for sarcopenia: plasma biomarkers of abrupt changes in physical activity. Metabolites 9. https://doi.org/10.3390/metabo9070134.
Schousboe, A., Scafidi, S., Bak, L.K., Waagepetersen, H.S., McKenna, M.C., 2014. Glutamate metabolism in the brain focusing on astrocytes. Adv. Neurobiol. 11, 13–30. https://doi.org/10.1007/978-3-319-08894-5_2.
Shivamurthy, V.K.N., Tahari, A.K., Marcus, C., Subramaniam, R.M., 2015. Brain FDG PET and the diagnosis of dementia. AJR Am. J. Roentgenol. 204, W76–W85. https://doi.org/10.2214/AJR.13.12363.
Siddik, M.A.B., Mullins, C.A., Kramer, A., Shah, H., Gannaban, R.B., Zabet-Moghaddam, M., Huebinger, R.M., Hegde, V.K., MohanKumar, S.M.J., MohanKumar, P.S., Shin, A.C., 2022. Branched-chain amino acids are linked with Alzheimer's disease-related pathology and cognitive deficits. Cells 11. https://doi.org/10.3390/cells11213523.
Smith, C.A., O'Maille, G., Want, E.J., Qin, C., Trauger, S.A., Brandon, T.R., Custodio, D. E., Abagyan, R., Siuzdak, G., 2005. METLIN: a metabolite mass spectral database. Ther. Drug Monit. 27, 747–751. https://doi.org/10.1097/01.ftd.0000179845.53213.39.
Snowden, S.G., Ebshiana, A.A., Hye, A., An, Y., Pletnikova, O., O'Brien, R., Troncoso, J., Legido-Quigley, C., Thambisetty, M., 2017. Association between fatty acid metabolism in the brain and Alzheimer disease neuropathology and cognitive performance: a nontargeted metabolomic study. PLoS Med. 14, e1002266 https://doi.org/10.1371/journal.pmed.1002266.
Ticinesi, A., Guerra, A., Nouvenne, A., Meschi, T., Maggi, S., 2023. Disentangling the complexity of nutrition, frailty and gut microbial pathways during aging: a focus on Hippuric acid. Nutrients 15. https://doi.org/10.3390/nu15051138.
Toledo, J.B., Arnold, M., Kastenmüller, G., Chang, R., Baillie, R.A., Han, X., Thambisetty, M., Tenenbaum, J.D., Suhre, K., Thompson, J.W., John-Williams, L.S., MahmoudianDehkordi, S., Rotroff, D.M., Jack, J.R., Motsinger-Reif, A., Risacher, S. L., Blach, C., Lucas, J.E., Massaro, T., Louie, G., Zhu, H., Dallmann, G., Klavins, K., Koal, T., Kim, S., Nho, K., Shen, L., Casanova, R., Varma, S., Legido-Quigley, C., Moseley, M.A., Zhu, K., Henrion, M.Y.R., van der Lee, S.J., Harms, A.C., Demirkan, A., Hankemeier, T., van Duijn, C.M., Trojanowski, J.Q., Shaw, L.M., Saykin, A.J., Weiner, M.W., Doraiswamy, P.M., Kaddurah-Daouk, R., 2017. Metabolic network failures in Alzheimer's disease: a biochemical road map. Alzheimers Dement. 13, 965–984. https://doi.org/10.1016/j.jalz.2017.01.020.
Trushina, E., Dutta, T., Persson, X.-M.T., Mielke, M.M., Petersen, R.C., 2013. Identification of altered metabolic pathways in plasma and CSF in mild cognitive impairment and Alzheimer's disease using metabolomics. PLoS One 8, 1–13. https://doi.org/10.1371/journal.pone.0063644.
Van Der Velpen, V., Teav, T., Gallart-Ayala, H., Mehl, F., Konz, I., Clark, C., Oikonomidi, A., Peyratout, G., Henry, H., Delorenzi, M., Ivanisevic, J., Popp, J., 2019. Systemic and central nervous system metabolic alterations in Alzheimer's disease. Alzheimers Res. Ther. 11, 1–12. https://doi.org/10.1186/s13195-019-0551-7.
Wang, D.-C., Sun, C.-H., Liu, L.-Y., Sun, X.-H., Jin, X.-W., Song, W.-L., Liu, X.-Q., Wan, X.-L., 2012. Serum fatty acid profiles using GC-MS and multivariate statistical analysis: potential biomarkers of Alzheimer's disease. Neurobiol. Aging 33, 1057–1066. https://doi.org/10.1016/j.neurobiolaging.2010.09.013.
Varma, V.R., Oommen, A.M., Varma, S., Casanova, R., An, Y., Andrews, R.M., O'Brien, R., Pletnikova, O., Troncoso, J.C., Toledo, J., Baillie, R., Arnold, M., Kastenmueller, G., Nho, K., Doraiswamy, P.M., Saykin, A.J., Kaddurah-Daouk, R., Legido-Quigley, C., Thambisetty, M., 2018. Brain and blood metabolite signatures of pathology and progression in Alzheimer disease: A targeted metabolomics study. PLoS Med 15, e1002482. https://doi.org/10.1371/journal.pmed.1002482.
Wang, H., Lian, K., Han, B., Wang, Y., Kuo, S.-H., Geng, Y., Qiang, J., Sun, M., Wang, M., 2014a. Age-related alterations in the metabolic profile in the hippocampus of the senescence-accelerated mouse prone 8: a spontaneous Alzheimer's disease mouse model. J. Alzheimers Dis. 39, 841–848. https://doi.org/10.3233/JAD-131463.
Wang, R.Y., Wilcox, W.R., Cederbaum, S.D., 2014b. Amino acid metabolism. In: Reference Module in Biomedical Sciences. Elsevier. https://doi.org/10.1016/B978-0-12-801238-3.05564-1.
Wang, G., Zhou, Y., Huang, F.-J., Tang, H.-D., Xu, X.-H., Liu, J.-J., Wang, Y., Deng, Y.-L., Ren, R.-J., Xu, W., Ma, J.-F., Zhang, Y.-N., Zhao, A.-H., Chen, S.-D., Jia, W., 2014c. Plasma metabolite profiles of Alzheimer's disease and mild cognitive impairment. J. Proteome Res. 13, 2649–2658. https://doi.org/10.1021/pr5000895.
Whiley, L., Sen, A., Heaton, J., Proitsi, P., García-Gómez, D., Leung, R., Smith, N., Thambisetty, M., Kloszewska, I., Mecocci, P., Soininen, H., Tsolaki, M., Vellas, B., Lovestone, S., Legido-Quigley, C., 2014. Evidence of altered phosphatidylcholine metabolism in Alzheimer's disease. Neurobiol. Aging 35, 271–278. https://doi.org/10.1016/j.neurobiolaging.2013.08.001.
Wilkins, J.M., Trushina, E., 2017. Application of metabolomics in Alzheimer's disease. Front. Neurol. 8, 719. https://doi.org/10.3389/fneur.2017.00719.
Wilson, D.M., Binder, L.I., 1997. Free fatty acids stimulate the polymerization of tau and amyloid β peptides: in vitro evidence for a common effector of pathogenesis in Alzheimer's disease. Am. J. Pathol. 150, 2181–2195.
Wishart, D.S., Feunang, Y.D., Marcu, A., Guo, A.C., Liang, K., Vázquez-Fresno, R., Sajed, T., Johnson, D., Li, C., Karu, N., Sayeeda, Z., Lo, E., Assempour, N., Berjanskii, M., Singhal, S., Arndt, D., Liang, Y., Badran, H., Grant, J., Serra-Cayuela, A., Liu, Y., Mandal, R., Neveu, V., Pon, A., Knox, C., Wilson, M., Manach, C., Scalbert, A., 2018. HMDB 4.0: the human metabolome database for 2018. Nucleic Acids Res. 46, D608–D617. https://doi.org/10.1093/nar/gkx1089.
Wood, P.L., Barnette, B.L., Kaye, J.A., Quinn, J.F., Woltjer, R.L., 2015a. Non-targeted lipidomics of CSF and frontal cortex grey and white matter in control, mild cognitive impairment, and Alzheimer's disease subjects. Acta Neuropsychiatr. 27, 270–278. https://doi.org/10.1017/neu.2015.18.
Wood, P.L., Medicherla, S., Sheikh, N., Terry, B., Phillipps, A., Kaye, J.A., Quinn, J.F., Woltjer, R.L., 2015b. Targeted Lipidomics of fontal cortex and plasma diacylglycerols (DAG) in mild cognitive impairment and Alzheimer's disease: validation of DAG accumulation early in the pathophysiology of Alzheimer's disease. J. Alzheimers Dis. 48, 537–546. https://doi.org/10.3233/JAD-150336.
World Medical Association, 2013. World medical association declaration of Helsinki: ethical principles for medical research involving human subjects. JAMA 310, 2191–2194. https://doi.org/10.1001/jama.2013.281053.
Wu, G., 2009. Amino acids: metabolism, functions, and nutrition. Amino Acids 37, 1–17. https://doi.org/10.1007/s00726-009-0269-0.
Yilmaz, A., Ugur, Z., Bisgin, H., Akyol, S., Bahado-Singh, R., Wilson, G., Imam, K., Maddens, M.E., Graham, S.F., 2020. Targeted metabolic profiling of urine highlights a potential biomarker panel for the diagnosis of Alzheimer's disease and mild cognitive impairment: a pilot study. Metabolites 10. https://doi.org/10.3390/metabo10090357.
Yin, C., Harms, A.C., Hankemeier, T., Kindt, A., de Lange, E.C.M., 2023. Status of Metabolomic measurement for insights in Alzheimer’s disease progression—what is missing? Int. J. Mol. Sci. 24 https://doi.org/10.3390/ijms24054960.
Zvěřová, M., 2019. Clinical aspects of Alzheimer's disease. Clin. Biochem. 72, 3–6. https://doi.org/10.1016/j.clinbiochem.2019.04.015.